PROJECT SQUID

TECHNICAL REPORT FIL-1-R

INVESTIGATION OF THE ATTENUATION OF SHOCK WAVES PROPAGATED THROUGH AN IONIZED GAS IN THE PRESENCE OF A TRANSVERSE MAGNETIC FIELD

by

S. P. Carfagno and G. P. Wachtell

FRANKLIN INSTITUTE LABORATORIES

Philadelphia, Pennsylvania.

Project SQUID is a cooperative program of basic research relating to Jet Propulsion. It is sponsored by the Office of Naval Research and is administered by Princeton University through Contract Nonr1858(25), NR-098-038.

June 1961

Technical Report FIL-1-R

PROJECT SQUID

A COOPERATIVE PROGRAM
OF FUNDAMENTAL RESEARCH
AS RELATED TO JET PROPULSION
OFFICE OF NAVAL RESEARCH, DEPARTMENT OF THE NAVY

Contract Nonr1858(25), NR-098-03

INVESTIGATION OF THE ATTENUATION OF SHOCK WAVES PROPAGATED THROUGH AN IONIZED GAS IN THE PRESENCE OF A TRANSVERSE MAGNETIC FIELD

by

S. P. Carfagno and G. P. Wachtell

Franklin Institute Laboratories

Philadelphia, Pennsylvania

June 1961

PROJECT SQUID HEADQUARTERS
JAMES FORRESTAL RESEARCH CENTER
PRINCETON UNIVERSITY
PRINCETON, NEW JERSEY

ABSTRACT

Measurements have been made of the attenuation of shock waves propagated through an ionized gas in the presence of a transverse magnetic field. Ionization was produced by maintaining a radio frequency discharge in the low pressure section of a shock tube. The electrical gas conductivity achieved by this means was less than 1 mho/m, a value much smaller than had been anticipated. Largely because of the low conductivity, negligible shock wave attenuations were predicted by the pertinent theory of magnetohydrodynamics (MHD). Nonetheless, appreciable shock wave attenuations were observed. Measurements made with several experimental arrangements and statistical analysis of the data demonstrate an MHD effect. A satisfactory explanation for the apparent discrepancy between theory and experiment was not attained, although some plausible speculations were made.

This report includes a discussion of MHD theory and the theory of a simple shock tube in addition to a detailed discussion of the experimental measurements and an analysis of the data.

Table of Contents

Illustrations

Tables

Symbols

a	speed of sound
A	cross-sectional area of shock tube
B	magnetic inductance
c	speed of light
C_v	specific heat capacity at constant volume
e	electron charge
E	electric field intensity
f	frequency
g	acceleration of gravity
h	enthalpy per unit mass
I_d	current through rf discharge
j	current density
ℓ	length of rf discharge in shock tube
L	length of magnetic field region
m	electron mass
n_a	number of atoms per unit volume in experimental gas before ionization
n_e	number of free electrons per unit volume
p	pressure
p_2	pressure behind incident shock wave
$P_{41} = p_4/p_1$	ratio of pressures across diaphragm in shock tube
R	universal gas constant
t	time
T	absolute temperature
u	gas speed
v	gas velocity
V_d	voltage across discharge electrodes

W_{11}		Mach number of incident shock wave
x, y, z		Cartesian coordinates
r, θ		cylindrical coordinates
α		shock wave attenuation parameter, defined in Section 5.2
β	=	n_e/n_a
μ		magnetic permeability of ionized gas
μ_o		magnetic permeability of free space
ρ		mass density
σ		electrical conductivity in presence of magnetic field
σ_o		electrical conductivity in absence of magnetic field
τ		mean time between collisions of electrons and neutral atoms
ω_e		Larmor frequency of electrons
∇	=	$\underline{i}\frac{\partial}{\partial x} + \underline{j}\frac{\partial}{\partial y} + \underline{k}\frac{\partial}{\partial z}$, where $\underline{i}$, $\underline{j}$, $\underline{k}$ are unit vectors in the x, y, z directions

1. INTRODUCTION

Magnetohydrodynamics (MHD) is the study of the motion of an electrically conductive fluid in the presence of a magnetic field. Motion of the fluid through the field induces currents which modify the field; at the same time the interaction of the field and induced currents produces mechanical forces which modify the motion. Thus, it is a study which involves the coupling of equations of electromagnetic theory with those of hydrodynamics. It has applications in astrophysics, controlled thermonuclear fusion, propulsion, and power generation, among others. Although activity in this field has exploded during the last few years, its roots go back many years.

Alpher[1] has recorded a number of interesting historical notes, a few of which are mentioned briefly here. As early as in 1832, Michael Faraday suggested that tidal motions of the conducting oceans are the source of changes in the earth's magnetic field, and he conducted a crude experiment in which he tried to correlate tidal motions of the River Thames with changes in the earth's magnetic field. In the same year, W. Ritchie pumped water by passing through it a current transverse to an applied magnetic field. The now familiar pinch phenomenon was observed as early as in 1907, when sufficiently large currents were passed through liquid metals. In 1937 J. Hartmann and F. Lazarus reported on magnetohydrodynamic effects on the velocity profile and transition from laminar to turbulent flow associated with the flow of mercury in a channel through a transverse magnetic field. A few years later H. Alfven

---

This work was sponsored by Project SQUID which is supported by the Office of Naval Research, Department of the Navy, under contract Nonr1858(25) NR-098-038. Reproduction in full or in part is permitted for any use of the United States Government.

originated the idea of the freezing together of fluid motion and magnetic field lines and predicted a new means of energy propagation: by wave motion along the magnetic field direction in fluids of high electrical conductivity. Subsequently, the existence of these Alfven waves was verified by S. Lundquist and B. Lehnert by experiments with mercury and liquid sodium.

From such beginnings have sprung the exotic experiments of today with plasmas at temperatures up to 100,000°K and magnetic fields of 100 kilogauss. Although interest was centered on MHD effects in "cosmic" problems during most of the development period, current interest in MHD is centered about controlled thermonuclear fusion, propulsion, and power generation.

2. THE EQUATIONS OF MAGNETOHYDRODYNAMICS

As we have already stated, MHD involves the interaction between a magnetic field and the motion of an electrically conductive fluid. The equations which are needed to describe MHD phenomena are thus a combination of the electromagnetic and hydrodynamic equations. The simplest equations are those based on a macroscopic point of view in which the fluid is considered to be continuous and to have such properties as viscosity and thermal and electrical conductivities. Such phenomena as the diffusion of the individual particles are neglected, and therefore the equations do not provide a complete description of the situation, particularly when the fluid is an ionized gas. However, the equations based on a one-component model provide a convenient starting point. The presentation given here follows closely the treatments by Cowling[2] and Sears[3].

Maxwell's displacement currents are assumed to be negligible and, consistent with this, it is also assumed that accumulation of electric charge is negligible and that electric currents flow in closed circuits. With these assumptions, in CGS units, the basic electromagnetic equations are:

$$\nabla \times \vec{B} = \frac{4\pi}{c}\vec{j} \tag{1}$$

$$\nabla \times \vec{E} = -\frac{1}{c}\frac{\partial \vec{B}}{\partial t} \tag{2}$$

$$\nabla \cdot \vec{j} = 0 \tag{3}$$

$$\nabla \cdot \vec{B} = 0 \tag{4}$$

If the material has velocity $\vec{v}$, there will be an induced emf $\vec{v} \times \vec{B}$, which is experienced by the fluid in addition to the applied field. Thus we can write a generalized Ohm's law

$$\vec{j} = \sigma(\vec{E} + \vec{v} \times \vec{B}) \qquad (5)$$

The hydrodynamic equation of continuity is applicable as it stands

$$\frac{\partial \rho}{\partial t} + \nabla \cdot (\rho \vec{v}) = 0 \qquad (6)$$

The momentum and energy equations, however, must be modified to account for phenomena which appear as a consequence of the conductivity of the fluid and the presence of electric and/or magnetic fields. The equation of motion must include the body force, $\vec{j} \times \vec{B}$ per unit volume

$$\rho \frac{d\vec{v}}{dt} = -\nabla p + \rho \vec{g} + \vec{F} + \vec{j} \times \vec{B} \qquad (7)$$

where $\rho \vec{g}$ is the body force per unit volume due to gravity, $\vec{F}$ represents the viscous forces per unit volume, and $^{d}/dt$ is the convective derivative

$$\frac{d}{dt} = \frac{\partial}{\partial t} + \vec{v} \cdot \nabla \qquad (8)$$

The energy equation is modified by addition of the term j^2/σ, which represents the Joule heating

$$C_v \rho \frac{dT}{dt} = p \frac{d\rho}{dt} + \frac{j^2}{\sigma} + Q \qquad (9)$$

where Q denotes all forms of heat added, exclusive of Joule heating.

When the fluid is a gas, it is useful to include the equation of state. For a perfect gas we have

$$p = \rho RT \qquad (10)$$

but in many applications which involve a high degree of dissociation and ionization, it is necessary to use a modification of the perfect gas law. If ionization of a monatomic gas is the only process involved, for example, one may multiply the right hand side of Equation 10 by $(1 + \beta)$, where β is the degree of ionization.

The above equations constitute the basic equations of magnetohydrodynamics. Except for very simple geometries their

solution requires some simplification. Before proceeding further, however, it will be interesting to discuss briefly some of the features which have resulted from the combination of hydrodynamic and electromagnetic equations.

The hydrodynamic equations have been modified by the body force $\vec{j} \times \vec{B}$ and the Joule heating j^2/σ; Ohm's law has been generalized by including the induced emf, $\vec{v} \times \vec{B}$. The body force is the familiar force acting on any conductor carrying a current in a magnetic field, such as we have in an electric motor. It is of particular interest when it occurs in a fluid, however, where gravity is normally the only body force. A specific example of the origin of this force and its effect is given in Section 3, where MHD interactions in a shock tube are discussed. The induced emf which arises when conductive fluids flow through a magnetic field is likewise no more than the familiar phenomenon which operates a generator. Even in the absence of applied electric fields, the induced emf can cause current flow, which in turn gives rise to the body force. The generalization of Ohm's law by including the induced emf, $\vec{v} \times \vec{B}$, is a correct approximation only for conductors that are electrically neutral. In the case of ionized gases (the experimental fluid discussed later) this is a very good approximation because the electrons and positive ions are never separated by more than extremely small distances. In Eqn. (5), the vector $\vec{E}$ should be understood to include the contribution due to charge separation. As described by Sears[3], we may say that to any small element of the fluid there is applied the emf, $\vec{v} \times \vec{B}$, plus that part of $\vec{E}$ due to effects exterior to the element. And we may consider that the potential drop $\vec{j}/\sigma$ through the element is diminished by the part of $\vec{E}$ that is due to charge separation.

3. MAGNETOHYDRODYNAMIC INTERACTION IN A SHOCK TUBE

In this Section we will consider the modification of shock wave motion in a shock tube when an MHD interaction occurs. (A brief description of the phenomena which occur in a simple shock tube is given in Appendix A.) Here, we will focus our attention on the flow behind the incident shock wave; the basic equations that hold in the absence of MHD effects will be written, and the manner of taking an MHD effect into account will be shown. The development of the basic equations may be found in a standard text on gasdynamics, such as Reference 7. We have followed References 8 and 9 in discussing the MHD effect.*

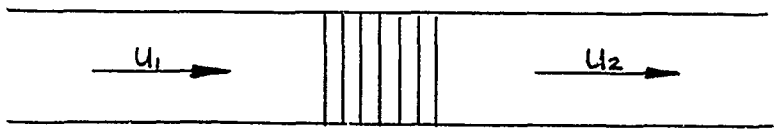

Figure 1. Flow through nonequilibrium region in constant area channel.

Let us consider adiabatic flow in a constant area channel in which two regions, 1 and 2 as shown in Fig. 1, are separated by a nonequilibrium region. Regardless of the size or nature of the nonequilibrium region, as long as no momentum is transferred to the exterior of the gas and the regions 1 and 2 are outside of it, the equations of continuity, momentum, and energy are:

---

* We describe here the type of analysis that was used in the course of the study. Improved theoretical treatments have become available recently. See, for example, Reference 22.

$$\rho_1 u_1 = \rho_2 u_2 \tag{11}$$

$$p_1 + \rho_1 u_1^2 = p_2 + \rho_2 u_2^2 \tag{12}$$

$$h_1 + u_1^2/2 = h_2 + u_2^2/2 \tag{13}$$

The nonequilibrium region may be a vanishingly thin region representing the discontinuity of a stationary shock wave. In that case, if we have a measure of the shock strength (e.g. the pressure ratio across it), the above equations can be used to derive the velocity and temperature ratios across the shock wave.

We wish to consider the situation when there is a magnetic field normal to the channel within the shaded region of Fig. 1, and an electrically conductive gas is flowing through the channel. In this case an MHD interaction occurs within the region of the magnetic field, and a modification of the momentum equation is required to account for the loss of momentum which occurs. It can be shown that this problem is similar to the problem of calculating the effect of an obstruction such as a screen located at a cross-section of the channel. In such problems one must add to the right side of the momentum equation a term representing the rate of delivery of momentum to the world external to the gas.

In the case chosen the gas velocity and magnetic field are normal to each other, so that the induced emf is uB and has a direction normal to both $\vec{v}_x$ and $\vec{B}$ as shown in Fig. 2. The induced emf will give rise to induced currents, provided that a closed circuit exists in which the currents can flow. (The matter of closing the current path is discussed further, below.) Finally, the induced currents interact with the applied field* to produce the electric body force

---

* We have assumed that the magnetic field associated with the induced currents is negligible in comparison with the applied field, i.e. the magnetic Reynolds number is small, as is true in experiments involving small electrical conductivity.

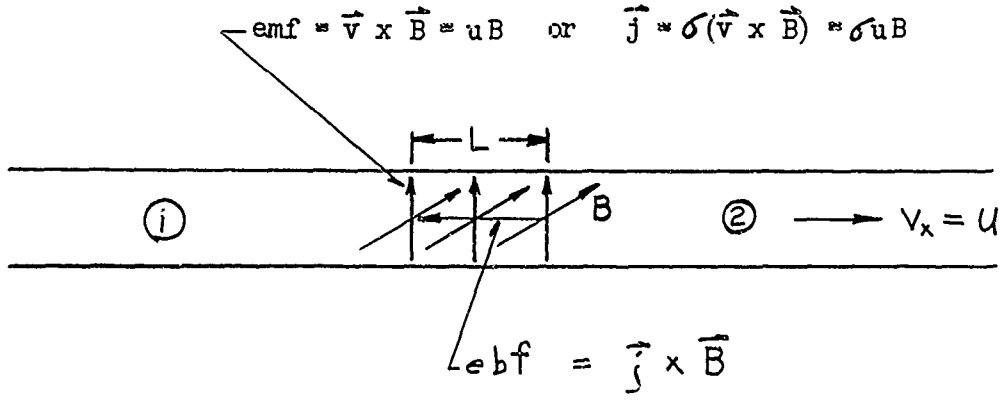

Figure 2. Region of magnetohydrodynamic interaction.

$\vec{j} \times \vec{B}$ (per unit volume). Integration of the "ebf" over the extent of the magnetic field gives us the total rate of change in momentum per unit cross-sectional area of the shock tube,

$$\Gamma = \int_0^L \vec{j} \times \vec{B} dx$$

This is a vector in the -x direction. Its magnitude, represents

$$\Gamma = \int_0^L \sigma u B^2 dx \qquad (14)$$

the rate of loss of momentum per unit area, and is taken into account by adding Γ to the right side of the momentum equation, Equation 12. The exact evaluation of the integral in Eqn. 14 is not easy because of the variation of the factors in the integrand, especially σ, over the distance L. A reasonable calculation can be made by assuming uniformity over the interaction region and assigning "average" values to the variables.

In our experiment, the flow was established by propagation of a shock wave through the gas in our shock tube. As described in Reference 8, the above MHD interaction has several consequences in such a situation. One effect is that the flow speed is driven toward

the sonic value. If the flow entering the interaction region is supersonic ($u_1 > a_1$, where a_1 is the speed of sound in Region 1) then the flow speed is decreased, $u_2 < u_1$; on the other hand, if the entering flow is subsonic ($u_1 < a_1$) we will have an increase in flow speed, $u_2 > u_1$. This is the same type of speed change that occurs when gas flowing in a channel encounters an obstruction equivalent to a constriction of the channel. In the most general case, the other consequences of the MHD interaction include attenuation of the shock wave transmitted through the interaction region, reflection of a shock wave back into the flow entering the interaction region, and generation of an expansion wave behind the transmitted shock. Of all these effects our apparatus was capable of detecting only the attenuation of the transmitted shock wave.

Lin's theory assumes that the induced currents discussed above do flow, and it is not concerned with their experimental realization. However, the very need to assure free flow for the induced currents presents one of the difficult problems encountered in any experimental investigation of the phenomena described. If the currents cannot flow there will occur a rapid polarization of the fluid; surface charges will build up on the tube walls in such a way as to oppose the induced electric field. When the fluid is an ionized gas, even if the channel walls are conductive, or properly located electrodes are placed inside the channel, the high resistivity of the cool boundary layer will have the effect of making the walls practically insulating. There exist schemes, however, for causing the induced currents to flow in closed circuits inside the gas, thus avoiding the problems associated with the use of electrodes to close the circuits outside the gas. The simplest experimental arrangement that achieves this end involves the use of an axially symmetric magnetic field as produced by a coil concentric with the axis of a cylindrical channel. The main component of the field, the axial

component, has no effect on the gas motions but the radial component in the fringe region of the field is normal to the gas velocity and generates an induced field in the $\vec{v}_x \times \vec{r}$, or tangential direction. Thus the induced currents can flow in closed loops inside the gas. The non-uniformity of conditions over a cross-section of the cylindrical tube can be largely overcome by using an annular tube, in which case the magnetic field can be produced by an electromagnet with its core inside the inner tube forming the annulus. Reference 10 describes experiments performed with this type of geometry; it also describes another special geometry, which achieves closed currents within the gas, and the experiments performed with it.

The theory which applies when the channel walls are non-conductive has been developed by deLeeuw in Reference 11, for the configuration discussed by Lin[8] and also for the configurations with an axially symmetric magnetic field, with a cylindrical channel of either circular, or annular cross-section. deLeeuw assumes, as does Lin, that the working fluid is a gas ionized by a strong shock wave. He assumes that the gas is in thermal equilibrium and employs a theory developed in Reference 6 to relate the degree of ionization to the pressure and temperature of the gas. In addition, he discards the simplification, adopted by Lin, of using ideal gas theory to determine the gas properties. We discuss below the physical significance of those parts of deLeeuws analysis which are most relevant to our experiment.

Consider the case in which a magnet is placed across a tube so that a transverse magnetic field exists over a short distance along the axis of the tube. At the edges of the magnetic field region the field strength decreases with axial distance from its center. If the tube walls are non-conductive there can be no current flow through them. Over the axial distance in which the magnetic field strength is constant this condition is satisfied by a balance between the electric field induced by motion of the conductive gas

through the magnetic field and the electric field of the surface charges. In the edge regions, however, where there is a magnetic field gradient, the density of surface charge varies with axial position. In these regions therefore, axial currents can occur near the wall, providing a means for closing the circuits for the induced currents. Consequently, in a non-conductive tube the electric body force will exist only in the regions of appreciable magnetic field gradients.

The large influence of non-conductive walls was demonstrated by deLeeuw with a numerical comparison of a typical case with a transverse magnetic field and the limiting case (saturated core) for the annular tube, in which the induced currents close within the gas. On a conservative basis, he found that the drag pressure is approximately sixty times greater with the annular geometry. Furthermore, deLeeuw gives data which compare the predictions of his theory with the corresponding predictions when real gas effects are neglected. He shows that use of the ideal gas simplification exaggerates the MHD effects and therefore provides an inadequate description of the phenomena.

4. DESCRIPTION OF EXPERIMENTS

4.1 Apparatus and general procedures.

The apparatus is centered about a 1 in. diameter shock tube, 8 ft. long. Overall and closeup views of the apparatus are shown in Figures 3 and 4, respectively. The driver section is a brass tube, 2 ft. long; and the experimental section is a pyrex pipe, 6 ft. long. Cellophane is the diaphragm material used to separate the two sections; a solenoid-operated plunger was used to puncture the diaphragm. A vacuum pump and several manometers were provided for evacuating the tube sections and filling them with gas to known pressures. Two external electrodes consisting of copper sleeves were placed about 30 in. apart on the glass section; one was connected to ground and the other to the plate of the oscillator tube in the rf generator. When the generator was turned on the rf electric field caused the gas in the glass section to become ionized. Permanent magnets were used to create a magnetic field of approximately 1000 gauss over a section up to 10 in. long in the region between the rf electrodes. In some of the experiments, metal plates were placed inside the shock tube in the region of the magnetic field in an attempt to collect induced currents.

The first three sources of rf power tried were each discarded in favor of a higher powered source before a satisfactory discharge was achieved. Initial experiments were performed with a 100w, 2Mc oscillator constructed in our laboratories, using a single GL-211 oscillator tube. A 300w medical Wappler Short Wave Diathermy instrument had poorer performance in spite of its higher power rating, possibly because of its simple half wave power supply section and the lack of filtering. A second-hand 1 kw induction heater, modified to operate at 6 Mc, generated considerably better discharges but was too unstable. With each of these instruments several types of discharge electrodes and various coupling arrangements were tried in attempting

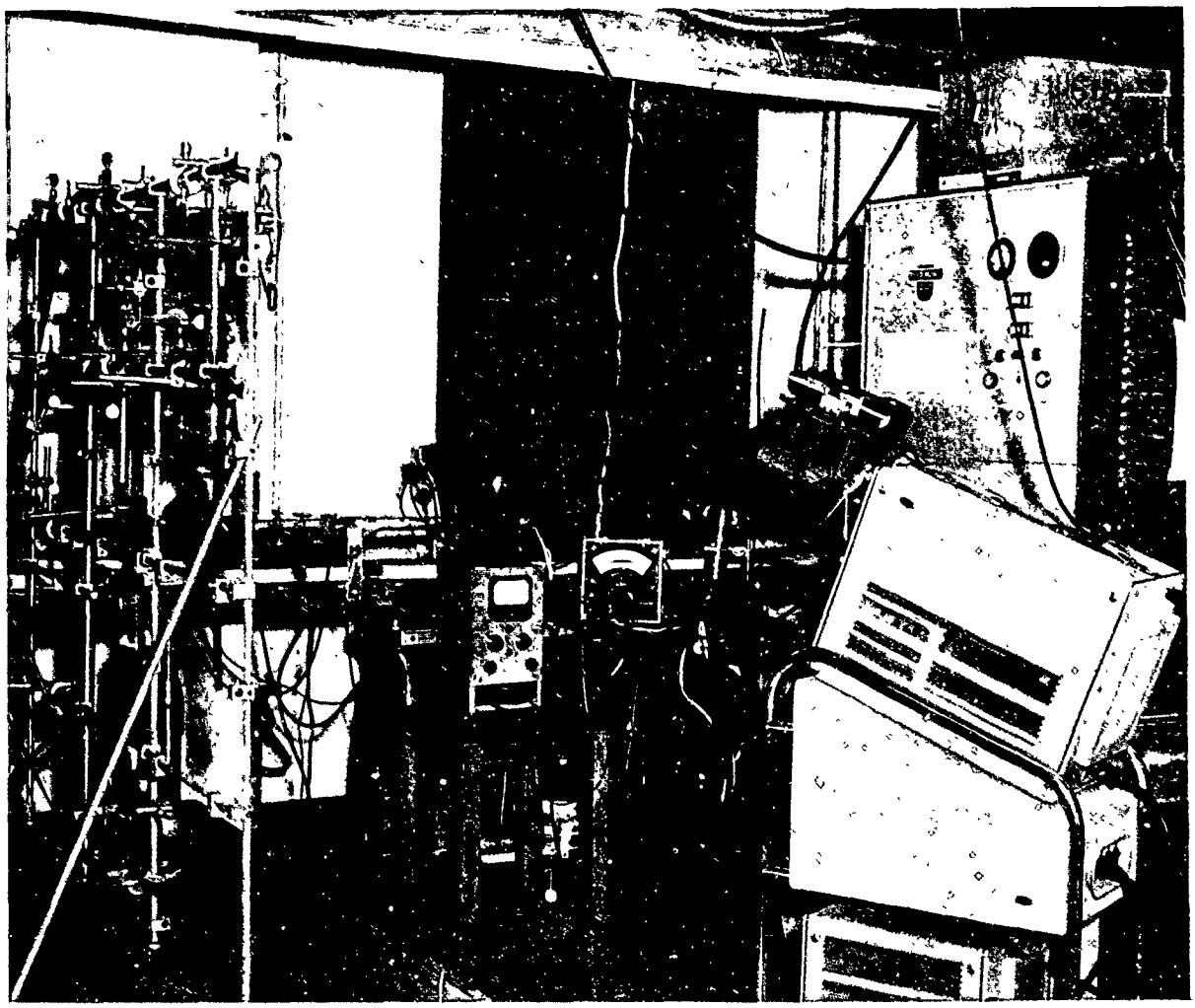

Figure 3. Overall View of Apparatus

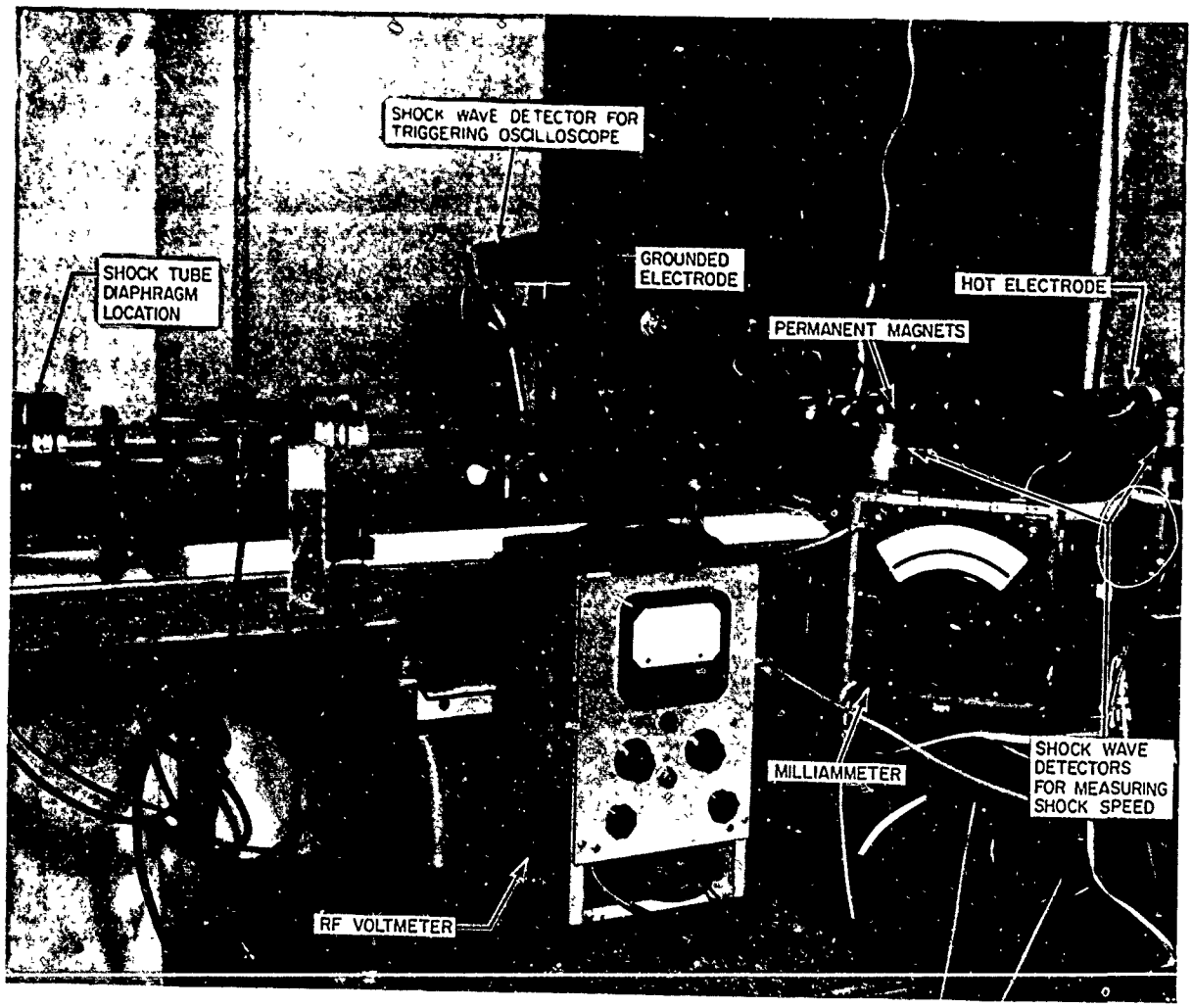

Figure 4. Closeup View of Experimental Section

to obtain a stable discharge with maximum power. Reference 15 and 16 describe this development phase in greater detail.

Reasonably satisfactory results were not obtained until we were able to use a 3 kw, 450 kc induction heater which had been acquired for another project. To some extent we experimented with several coupling arrangements; but, as with the 1 kw unit, we found that direct tank coupling worked best. The electrodes settled upon for routine use were 5 in. wide sleeves of 0.010 in. thick copper, having a close fit on the outside of the glass tube. It was necessary to insulate the hot electrode from the glass tube with a layer of Teflon in order to prevent sparking and the possibility of tube fracture due to pinpoint heating. It became possible, with the 3 kw unit, to maintain a discharge at pressures exceeding those possible with any of the other units. At the lower pressures, on the order of 1 mm Hg, the discharge appeared to extend to the walls of the tube and to be uniform over any cross-section. It was also possible to maintain a discharge over a much greater length of tube (up to 6 ft.) than was possible with the other rf generators tried.

Several measurements were made in a typical experiment, the most important of which was a measurement of the speed of the shock wave. This was done by exhibiting signals from two shock wave detectors, separated by a known distance, on a time-calibrated oscilloscope sweep. The detectors consisted of photomultiplier tubes sighted through two small holes on a line normal to the shock tube axis; signals were produced by the change in discharge intensity on arrival of the shock wave at the points viewed by the detectors. Other measurements included the discharge current, voltage on the hot electrode, rf generator plate current, and voltage on collector electrodes.

Initially the experiments were performed with room air as the working gas; later, most of the experiments were performed with argon obtained in a commercial cylinder. Typically, the pressure in

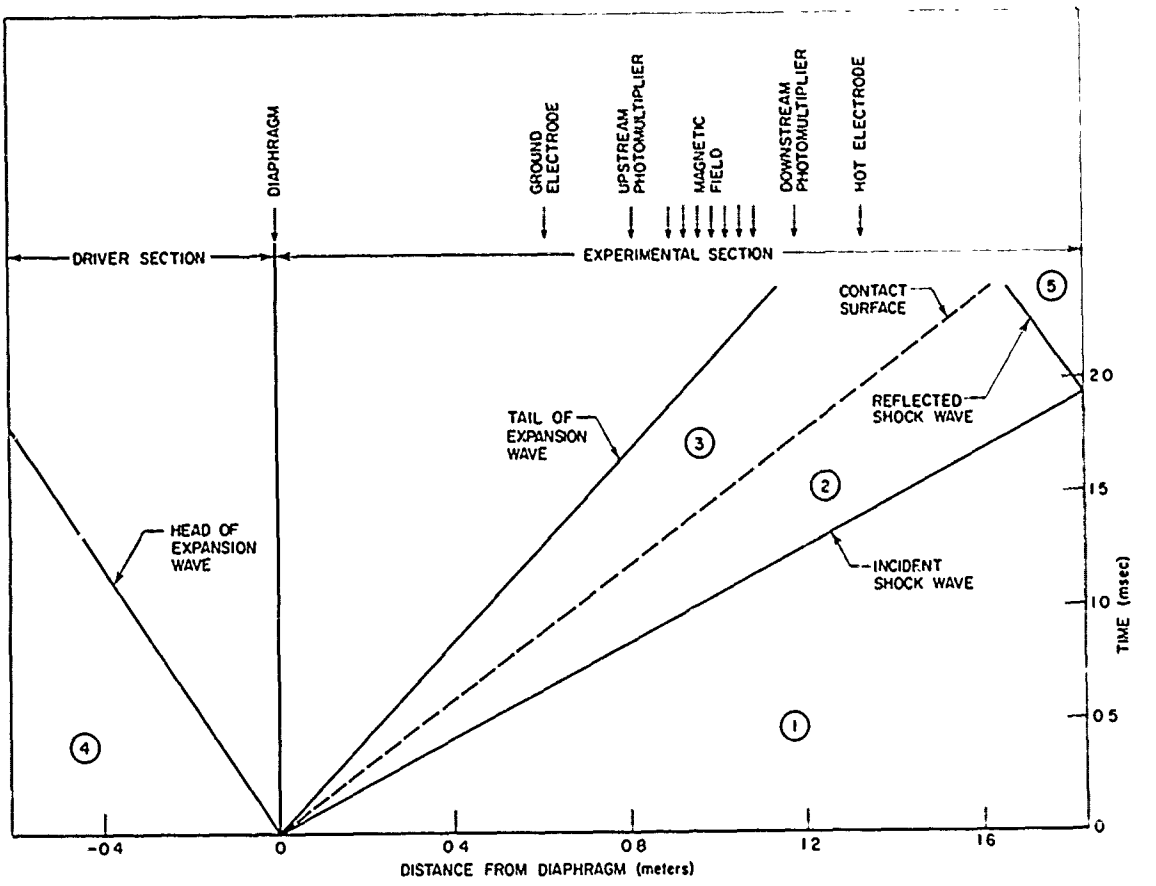

Figure 5. Typical Wave Diagram for Shock Tube Used in MHD Experiments.

Initial conditions: Air in both sections of tube.
$P_4/P_1 = 300$
$T_4 = T_1 = 300°K$

Calculated results: W_{11} = Mach number of incident shock wave = 2.75
$P_2 = P_3 = 8.65P_1$
$T_2 = 723°K$
$T_3 = 107°K$
$T_5 = 1178°K$ (assuming variable specific heat)

the glass section was 1 mm Hg, and in the driver section it was about 30 cm Hg. Thus, the pressure ratio P_{41}, across the diaphragm was on the order of 300. For the case in which both driver and driven sections of the shock tube were filled with air, and with $P_{41} = 300$, Fig. 5 gives a wave diagram, such as is described in Appendix A. The approximate location of electrodes, magnetic field, and photomultipliers is also shown in Fig. 5. This type of diagram aided in correlating photomultiplier signals with specific events in the shock tube.

4.2 Description of Experimental Measurements

Having described the apparatus and general procedure, we wish now to describe the specific experimental measurements that were made.

Figures 6 to 11 exhibit the oscilloscope traces that were obtained in various tests and also, in some cases, sketches of the experimental arrangement. The text accompanying each of these figures describes the object of the measurements and the procedures for making them. A summary discussion of all the tests precedes their individual description.

Some of the measurements provided general information concerning the discharge. In a typical experiment the rf voltage applied to the discharge electrodes remained approximately constant in amplitude regardless of changes in the discharge, ranging from maximum intensity to extinction. Because of their large magnitude, electrode voltages had to be attenuated to be exhibited on an oscilloscope screen. A resistive divider gave erroneous results because of the effect of stray capacitance. The difficulty was eliminated by using a capacitative divider. The discharge current was found to lead the voltage (by approximately sixty electrical degrees) as was to be expected on account of the capacitative coupling between rf generator and discharge.

Two collecting plates were placed opposite each other in the magnetic field region, for the purpose of collecting transverse currents, if such were generated by any means. The potential at the plates was dependent upon conditions within the tube: With a uniform discharge the collecting plate potential was approximately half the potential on the hot discharge electrode, as was to be expected from the location of the plates, midway between the discharge electrodes. When a shock wave was propagated through the discharge the portion upstream of the discharge was extinguished, at least partially. This caused the collecting plate potential to increase to a larger fraction of the voltage on the hot electrode, which was on the downstream side.

A harmonic component was noticed on some of the signals. Superimposed on the sinusoidal current wave form we noticed a harmonic signal with a frequency 24 times the fundamental rf frequency (f_o = 560 kc) and an amplitude about 10 percent that of the fundamental. A harmonic of twice this frequency, i.e. 48 x f_o, was observed superimposed on the collecting plate voltage when the gas pressure was 1 atm, which was too high for ionization to occur. If the hot electrode voltage had a similar harmonic component it was too small to be distinguished. We have not learned the cause of these high frequency components. They do not appear to be related to the electron collision frequency which is of order 10^{10} sec^{-1}. The Larmor frequencies of electrons and ions are irrelevant because the signals were observed in the absence of a magnetic field.

Simultaneous observation of discharge current and discharge radiation (as seen by a photomultiplier tube) showed that these two signals were approximately proportional to one another when conditions were uniform throughout the discharge. These signals helped provide an analysis of events when the diaphragm was ruptured and a shock wave was generated. The current was observed to decrease smoothly to zero. The radiation signals were more complicated; but generally, radiation was observed to decrease both upstream and downstream of the shock

wave, although the radiation level was always higher at downstream locations. Superimposed on the decreasing radiation signals there were sudden downward jumps which occurred when the shock wave passed through the section of discharge viewed. From these observations we may form the following picture of events. The shock wave raises the gas pressure and causes rapid deionization. At any instant, therefore, the section of discharge upstream of the shock wave will be less intense than the downstream portion. The discharge has a high impedance per unit distance, along the tube, behind the shock wave and, a low impedance per unit length ahead of the shock wave. Because the length of the upstream portion increases as the shock wave moves downstream, the total impedance increases with time; and the discharge current decreases with time. The continuous fall of discharge current affects both portions of the discharge continuously until it is extinguished. In other words, there is an additional contribution to the increase of total discharge impedance from a continuous increase of impedance per unit length in both portions of the discharge.

The photomultiplier signals had other features which were correlated with events of lesser importance, such as passage of diaphragm particles, the expansion wave, and the reflected shock wave through the section observed. These are discussed in conjunction with specific signal traces in the figures presented below.

If a direct current flowed between the collecting plates, as might happen if an MHD interaction occurred, there should have been a DC potential difference between the plates, superimposed on the rf voltage. An attempt was made to detect such a DC potential on an oscilloscope by connecting the plates to a differential amplifier. Although we obtained signals having features that could be correlated with events in the shock tube there was no evidence of currents induced by an MHD, or any other, interaction. These measurements were not conclusive because the unavoidably high impedance of the external circuitry may have precluded detection of small DC currents.

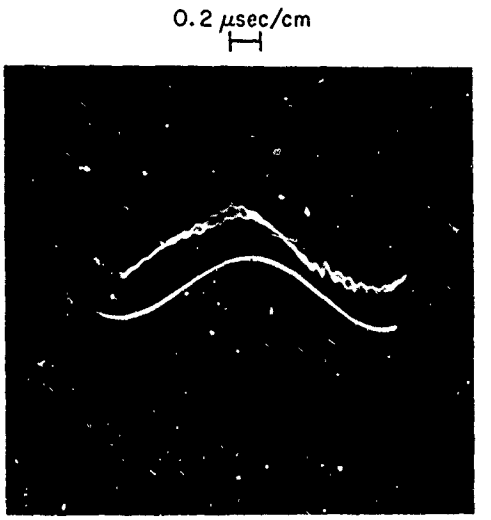

Figure 6 — Discharge voltage and current.
(Gas = argon at about 1 mm Hg pressure)

Upper Trace - Discharge current as indicated by potential drop across 10.45 ohm resistor in series with grounded electrode. (I_d = 75 ma)

Lower Trace - Discharge voltage as taken from hot electrode through resistive divider.

Current leads voltage by 25 electrical degrees.

A discussion of the individual experimental arrangements and measurements follows below. The data that were obtained is considered in the next Section.

A number of measurements were made on the rf discharge maintained in the glass section of the shock tube under steady conditions in order to determine some of the properties of the discharge. Fig. 6 shows the voltage and current wave forms as exhibited on a dual gun oscilloscope screen. The period is approximately 1.8 μ sec, corresponding to a frequency of about 560 kc. Superimposed on the current there was observed a small signal of undetermined cause, whose frequency is approximately 24 times the fundamental frequency. From the time displacement of the peaks of the voltage and current forms it was determined that the current leads the voltage by approximately 25 electrical degrees. Because the voltage is capacitatively coupled to the discharge it was to be expected that the current would lead the voltage; however, as explained below, the measured phase difference was not correct in the experiment depicted in Fig. 6. Later experiments led us to the conclusion that stray shunt capacitance in the resistive divider used on the voltage signal caused the phase of the voltage wave to be shifted an unknown amount with respect to the current wave. In addition, stray capacitance caused the divider ratio to be radically different from the resistance ratio. For these reasons the resistive divider was replaced by a capacitative divider. Using this divider the phase difference was redetermined and found to be about 60 electrical degrees. Except for their horizontal displacement, the current and voltage signals were similar to those in Fig. 6, which was used because a picture of the correct traces was not available.

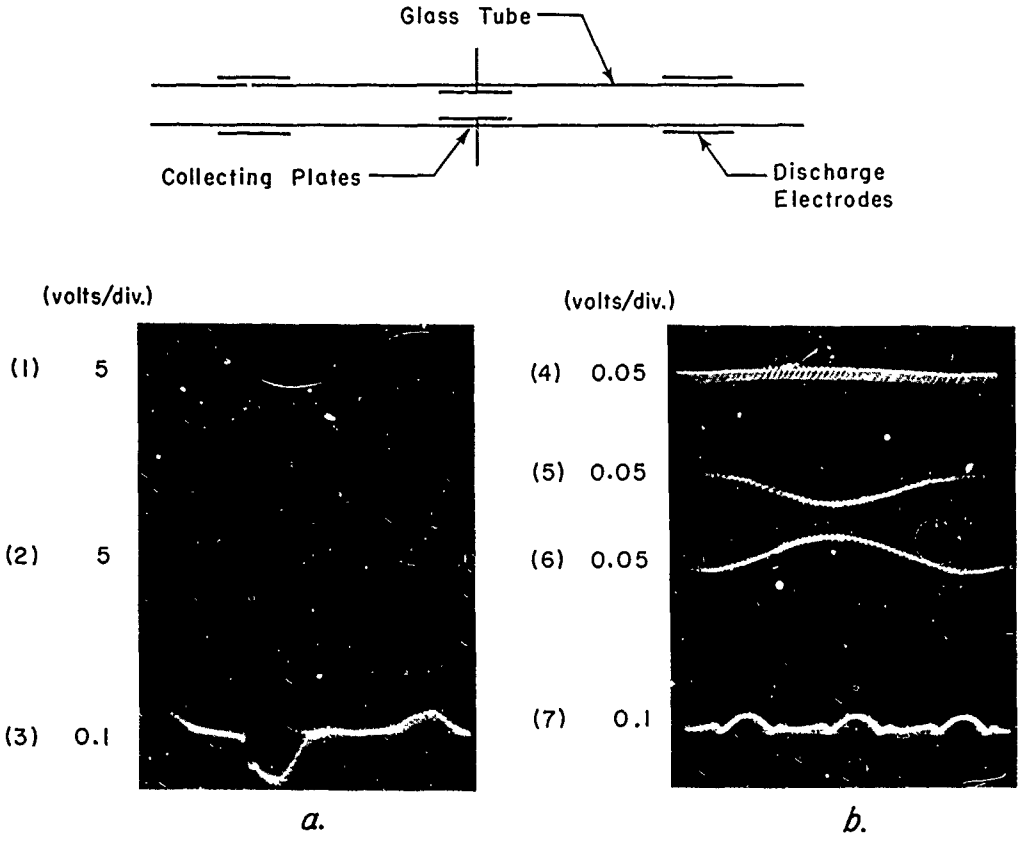

Figure 7 Collecting plate signals.

Variable capacitative divider adjusted for minimum amplitude of difference signal.

a. Air at 1/2 mm Hg pressure, I_d = 110 ma.
   (1) Voltage on one plate.
   (2) Voltage on other plate, inverted.
   (3) Difference of plate voltages, or sum of (1) and (2).

b. Air at 1 atm. pressure. No ionization produced by rf field.
   (4) Difference of plate voltages, or sum of (5) and (6).
   (5) Voltage on one plate.
   (6) Voltage on other plate, inverted.

   Air at 0.45 mm Hg pressure, I_d = 90 ma.
   (7) Both inputs of differential amplifier connected to bottom plate.

In a number of experiments we attempted to observe currents induced by the MHD effect. Two stainless steel plates, 1 in. x 5 in., were placed opposite each other inside the glass section of the shock tube as indicated in the sketch at the top of Fig. 7. The plates were shaped to the inner contour of the tube and connected to external leads directly through the glass wall. The leads were connected through a double, capacitative voltage divider to a differential amplifier. The divider had variable capacitors which were adjusted for equal attenuation of the signals from each plate. The plate signals resulting when a steady discharge was maintained are shown in Fig. 7a. The attenuated signals of each plate appear to be sinusoidal, but the difference signal has a complicated shape. The amplitude of the difference signal was approximately 2% of the amplitude of the signal on either plate when the capacitative divider was adjusted for minimum difference signal. In signal (7) of Fig. 7b, we see that, even when both leads were connected to the same plate, the differential amplifier did not have zero output. It is believed that the non-zero difference signal results from lack of identical attenuation in the two sections of the differential amplifier for high frequency (560 kc) signals.

Signals (4), (5), and (6), in Fig. 7b, are the difference and individual collecting plate signals for a case in which the pressure was so high (1 atm) that the rf generator was unable to maintain a discharge. In the presence of a discharge the collecting plates are closely coupled to the applied rf voltage, and the voltage on the plates was observed to be approximately half the applied voltage. However, the poor coupling in the absence of a discharge lowered the collecting plate voltage by a factor of approximately 100. We notice that in this case a small signal, whose frequency is 48 times the fundamental frequency, is superimposed upon the voltage signal. This is presumably related to the signal of frequency 24 times the fundamental seen superimposed on the current trace in Fig. 6.

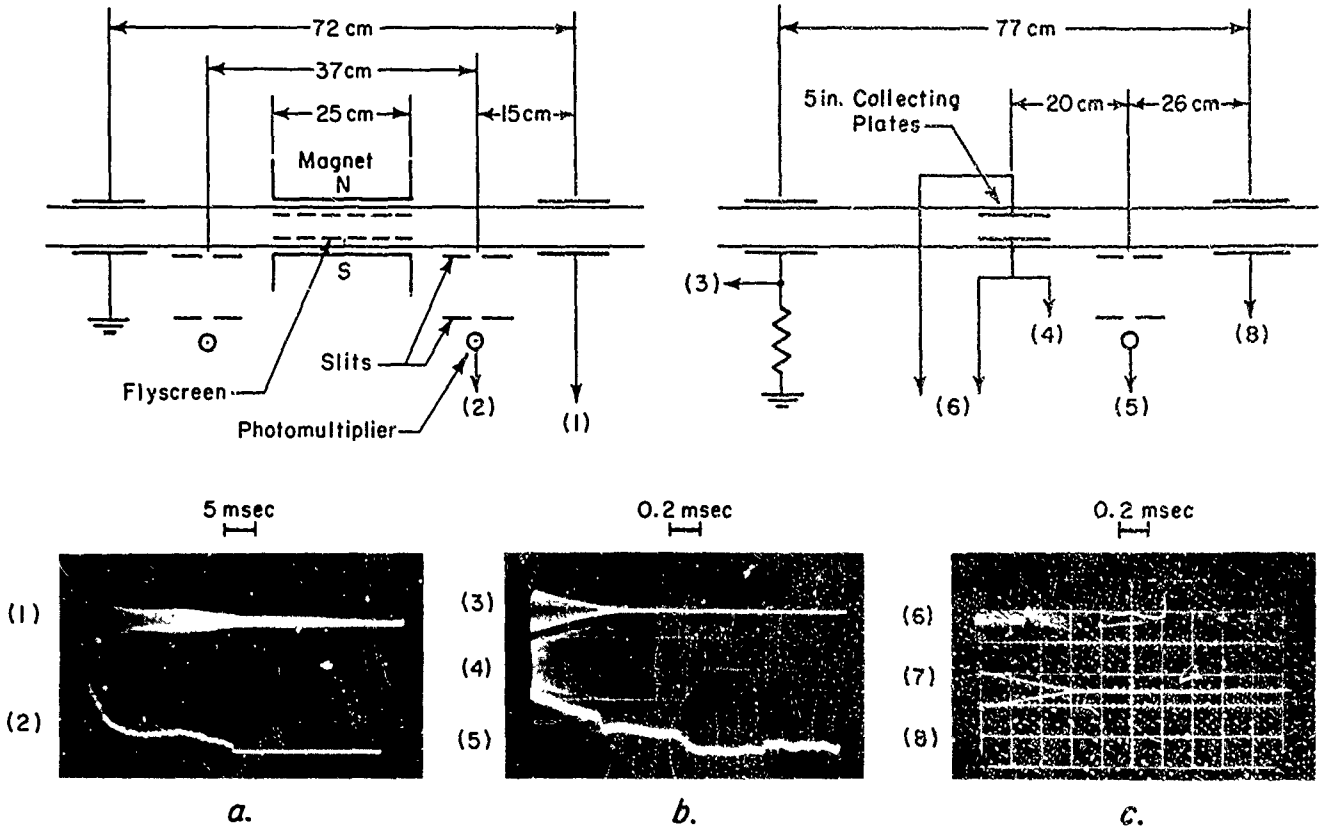

FIGURE 8 DECAY OF DISCHARGE

a. Decay of discharge when plate voltage switch on oscillator tube turned off. (Gas = air; $P_1 \sim 1$ mm Hg; V_d = 900 v, I_d = 75 ma before switch turned off, B = 1000 gauss)

(1) Voltage on hot electrode, taken from resistive divider.
(2) Discharge radiation viewed by 931A photomultiplier tube.

b. Decay of discharge on passage of shock wave. (Gas = argon, P_1 = 0.70 mm Hg, W_{11} = 2.52; V_d = 2240 v, I_d = 235 ma before shock passage)

(3) Discharge current, indicated by drop across 10.45 ohm, carbon resistor.
(4) Voltage on lower collecting plate, taken from capacitative divider.
(5) Discharge radiation viewed by photomultiplier. Downward swing at 0.4 msec indicates passage of shock wave past photomultiplier station.

c. Decay of discharge on passage of shock wave. (Gas = argon, P_1 = 0.88 mm Hg, W_{11} = 2.49; V_d = 2700 v, I_d = 215 ma before shock passage)

(6) Difference voltage from collecting plates.
(7) Same as (3).
(8) Voltage on hot electrode, taken from capacitative divider.

Fig. 8 shows the results of three experiments in which the nature of discharge decay was observed. Signals (1) and (2) in Fig. 8a were obtained with the arrangement shown in the upper left of the figure. A switch was opened to remove plate voltage from the oscillator tube of the induction generator; and the decay of voltage on the electrode connected to the oscillator tube plate and the decay of discharge intensity were observed simultaneously. The sweep speed in these experiments was comparatively slow, and therefore only the envelope of current and voltage signals was exhibited. It is interesting to note that the voltage decays with what appears to be a 60 cycles/sec pulsation, and that a corresponding pulsation occurs in the fall of discharge intensity as observed with a photomultiplier. Figures 8b and 8c were obtained with the arrangement shown in the upper right of the figure. In both cases the decay was caused by passage of a shock wave (from left to right) which raised the pressure beyond the limit at which the induction generator was capable of maintaining the discharge. Signals (3) and (7) exhibit the relatively smooth decay of discharge current. Signal (5) represents the discharge radiation as viewed by a photomultiplier at a station between the collecting plates and the hot electrode. The sharp downward swing of this signal at 0.4 msec indicates passage of the shock wave through the section viewed by the photomultiplier and serves to orient the time of events. Signal (8) shows that the voltage applied to the external discharge electrodes remained constant throughout the duration of the two experiments shown in b and c. The potential at the collecting plates, however, as shown by signal (4), increased to a maximum while the discharge current decreased to zero; thereafter, the beginning of a pulsation is noticed. The signal lacks symmetry about the horizontal base line because of beam blanking in the lower third of the oscilloscope screen. Signal (6) is that obtained from a differential amplifier to which the collecting plates were connected. The beginning of this signal appears to be the envelope of the type of signal seen in

trace (3) of Fig. 7a. A jump occurs at about the time the shock wave is passing through the collecting plate region, and thereafter the difference signal undergoes erratic modulation of larger amplitude. The jump cannot be attributed to an MHD effect because the magnetic field was absent. The erratic modulation is probably caused by lack of symmetry in the gas flow behind the shock wave. Although the amplitude of the difference signal is much greater during flow conditions than during the non-flow conditions preceding arrival of the shock wave, the difference amplitude is always a very small fraction of the amplitude of the practically equal signals on each collecting plate.

In summary, Figures 8b and 8c indicate that, in a typical experiment, the potential across the external discharge electrodes remains constant and the discharge current falls to zero relatively smoothly as the shock wave propagates through the ionized gas. When the shock wave is in a position between the discharge electrodes we may consider the discharge as constituting two impedances in series: there is a high impedance behind the shock wave where the degree of ionization has been decreased (possibly to zero), and there is a low impedance downstream of the shock wave where the discharge has been relatively less affected. Thus the total impedance between electrodes increases with time and the discharge current decreases with time. This picture of the experiment makes it understandable that the portion of discharge downstream of the shock wave should undergo a decrease in intensity. This is indicated by the fall of photomultiplier signal (5), preceding arrival of the shock wave at the station viewed.

THIS PAGE LEFT BLANK PURPOSELY.

a. *b.* *c.* *d.*

P_1 (mm Hg)	0.72	0.43	0.49	0.57
W_{11}	2.31	2.68	2.62	2.56
I_d (ma)	92	65	62	80
Magnetic Field	None	5 magnets; adjacent magnets aligned with fields in opposite directions	5 magnets common alignment	5 magnets common alignment
Screen*	No	No	No	Yes

FIGURE 9 Photomultiplier signals in shock tube experiments.

Arrangement same as in Figure 8a . Strength of magnets about 1000 gauss.

Upper trace - Discharge radiation viewed by upstream photomultiplier.

Lower trace - Discharge radiation viewed by downstream photomultiplier.

* Ten inch tube made of fly screen placed inside shock tube in region of magnetic field. In frame d, the rf field did not succeed in ionizing the gas in middle of screen tube.

The type of signals that were used to measure the shock speed is shown in Fig. 9. Having discussed the discharge behavior during shock passage with reference to Fig. 8, it is easy to explain the general features of the signals. Both upstream and downstream photomultipliers observe decreasing discharge radiation, with sudden falls occurring at the instants of shock passage through the viewing stations. In Fig. 9a, for example, the sudden falls in intensity can be seen at 0.7 msec and 1.2 msec. Some of the detailed features of the signals, however, are not as easily explained. Most of the upstream photomultiplier signals display a fairly rapid partial recovery of discharge intensity immediately following shock passage. A possible explanation is that some reionization occurs in the gas whose degree of ionization has been decreased by the sudden rise in pressure associated with the shock wave.

It is not known what might have caused the two dips in the downstream photomultiplier signal, seen in Fig. 9b, preceding the arrival of the shock wave at 0.7 msec. In the same signal, the spike beginning at 1.6 msec. might be associated with arrival of an expansion wave (generated in the driver gas when the diaphragm is ruptured) into the vicinity of the hot electrode. The signal rise may occur as a result of ionization that is permitted by the lowering of pressure; and the signal's disappearance is very likely caused by arrival of the reflected shock wave, which raises the pressure again. That the above is a reasonable explanation has been checked by determining the approximate times for the expansion wave and reflected shock wave to arrive at the vicinity of the hot electrode (with the aid of a wave diagram such as Fig. 5) and finding that these correspond approximately to the beginning and end, respectively, of the signal.

Finally, we can offer an explanation for the rise in downstream photomultiplier signal observed following shock passage, beginning at 0.8 msec in Fig. 9d. Visual observation of the discharge under the conditions of this experiment, in which a metal screen was

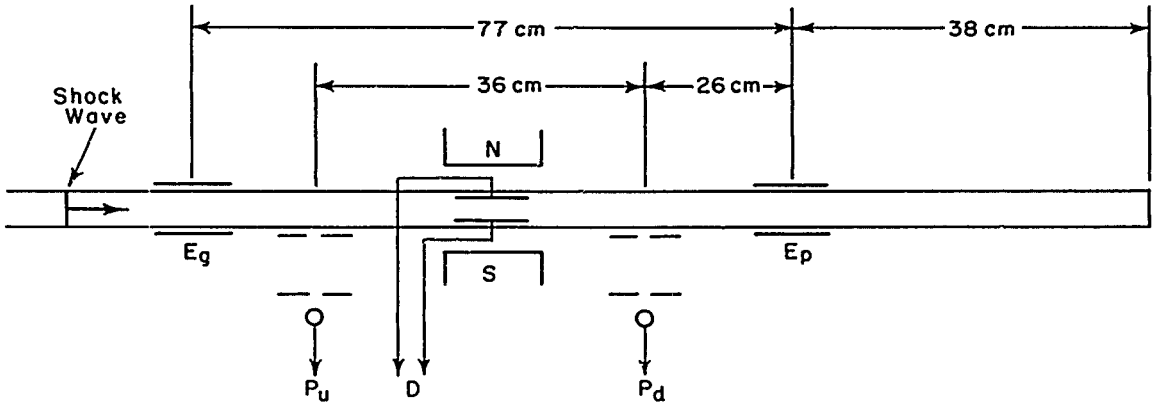

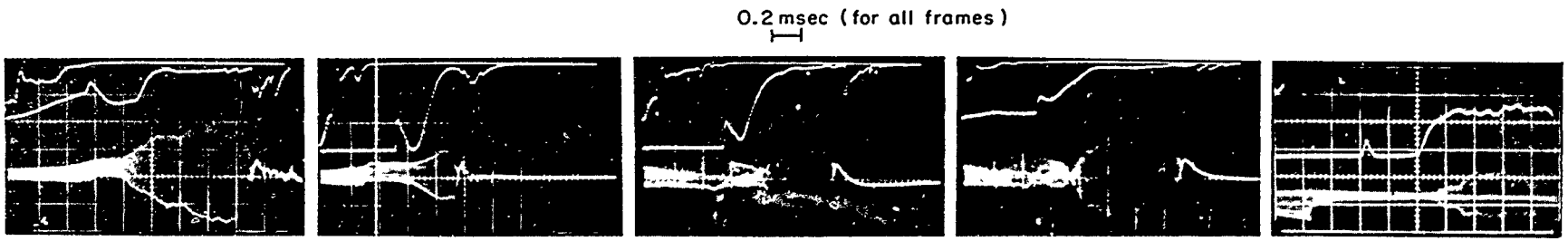

	a.	*b.*	*c.*	*d.*	*e.*
P_1 (mm Hg)	0.77	0.93	0.83	0.60	0.8
W_{11}	2.46	2.41	2.45	2.54	2.49
I_d (ma)	220	180	145	155	122
Magnets Present (1000 gauss)	No	No	Yes	Yes	No

Figure 10 Collecting plate signals. (E_g = grounded electrode, E_p = hot electrode, gas = argon)
Upper Trace - Discharge radiation as seen by upstream photomultiplier, P_u.
Middle Trace - Discharge radiation as seen by downstream photomultiplier, P_d.
Lower Trace - Difference voltage from collecting plates.
a,b,c,d - Plates connected to differential amplifier through Tektronix 10:1 attenuator probes.
e - Plates connected to differential amplifier through adjustable capacitative voltage dividers.

inserted in the magnetic field region, revealed that a residual discharge of small diameter extended from the hot electrode to the metal screen, following the experiment. This residual discharge remained as long as the induction generator was kept on. This rod-like discharge was not steady, however, it being observed to "snake" about inside the tube. It is thought, therefore, that the signal rise mentioned above results from the radiation of this unsteady residual discharge.

The difference signal from the collecting plates is shown in Fig. 10, for various experimental conditions, with and without a magnetic field present. These signals are similar to trace (6) in Fig. 8c, discussed above. The upstream and downstream photomultiplier signals are also displayed. Unlike the situation in the preceding figures, however, a decrease in discharge radiation is here indicated by a positive signal. The upstream photomultiplier signals are similar to those shown in Fig. 9. The downstream photomultiplier signals, however, following the sudden intensity decrease that occurs on shock passage, exhibit a more pronounced increase in discharge intensity than seen in Fig. 9. This is probably associated with the presence of the collecting electrodes, which were absent in the experiments of Fig. 9. The explanation is similar to that given for the intensity increase observed in Fig. 9d, which corresponded to a case in which a metal screen was inserted into the tube in approximately the same location as the position of the collecting plates in the experiments of Fig. 10. In the present case the discharge was reestablished between hot electrode and collecting plates, following shock passage. In other words, at the higher pressure behind the shock wave, the induction generator was not capable of maintaining the discharge the entire distance between hot and grounded electrodes; therefore, the nearer collecting plates became ground electrodes effectively.

The second rise in discharge intensity observed at the downstream location, 0.5 to 1.2 msec after shock passage, appears to be associated with arrival of an expansion wave at the vicinity of the hot electrode, as described in conjunction with Fig. 9b.

The bottom trace in each frame of Fig. 10 is the envelope of the difference between the upper and lower collecting plate voltages. In other words, they are the envelopes of signals such as (3), (4), and (7), shown in Fig. 7. In all cases except frame e, the plates were connected to a differential amplifier through 10:1 attenuator probes. In frame e an attempt was made to guarantee equal, total attenuation of each plate signal by using the capacitative voltage divider mentioned in Fig. 7, adjusted for minimum difference signal. No significant improvement was achieved by this technique, however.

The general features of the envelopes might be explained as follows: There are three main parts in the traces; a portion of medium amplitude is followed by a portion of large amplitude and the final portion has small amplitude. The final portion in frame e appears to have occurred off scope. The medium amplitude beginning appears to correspond to the low pressure signal of type (3) shown in Fig. 7. The beginning of the large amplitude portion can be correlated with arrival of the contact surface in the collecting plate region. Pieces of the ruptured cellophane diaphragm are carried in this portion of the gas stream and the non-symmetries established by their presence might account for the larger difference signals observed. The end of the large amplitude portion appears to coincide with reestablishment of the discharge between collecting plates and hot electrode. Playing the role of ground electrodes, the plates are likely to have more nearly the same potential — hence, the low difference signal. The beginning of the small amplitude portion has a DC shift for which a suitable explanation has not been found. It is always in the same direction and does not

depend on the presence of a magnetic field except insofar as this part of the signal was smoother when a magnetic field was present (frames c and d). Thus, we appear to be able to provide a reasonable explanation of the collecting plate signals, but there is no evidence that a DC induced current is collected by them while the electrically conductive gas is travelling through the collecting plate region, whether or not there is a transverse magnetic field present. This is not to say that these experiments prove the absence of induced currents: it is quite possible that the high impedance of the circuitry precluded the detection of currents.

In the experiments that have been described, a single measurement of shock speed was made during the interval of its travel between two photomultiplier detectors. In order to determine the effect on shock speed of various changes in experimental variables, such as the magnetic field, it was necessary to repeat experiments with all conditions constant, as nearly as possible, except for the one variable whose effect was to be determined. Because of the obvious advantages of being able to determine the effect of a given variable within a given experiment, the arrangement shown in Fig. 11 was tried. Four photomultiplier detectors were mounted so that a measure of shock speed could be obtained for three regions of its travel: the magnetic field region and the regions upstream and downstream of the magnetic field. The object of experiments with this arrangement was to see whether MHD effects within the magnetic field region could be detected in terms of shock speed attenuation.

The photomultiplier signals are similar to those described in Fig. 9, except that the polarity was reversed -- so that an upward swing indicates a decrease in discharge radiation. The necessity of using electronic choppers in order to display the four signals simultaneously on a single oscilloscope resulted in generally poor signals. The breaks indicating shock detection were difficult to locate accurately. In frame a, the breaks can be seen at approximately

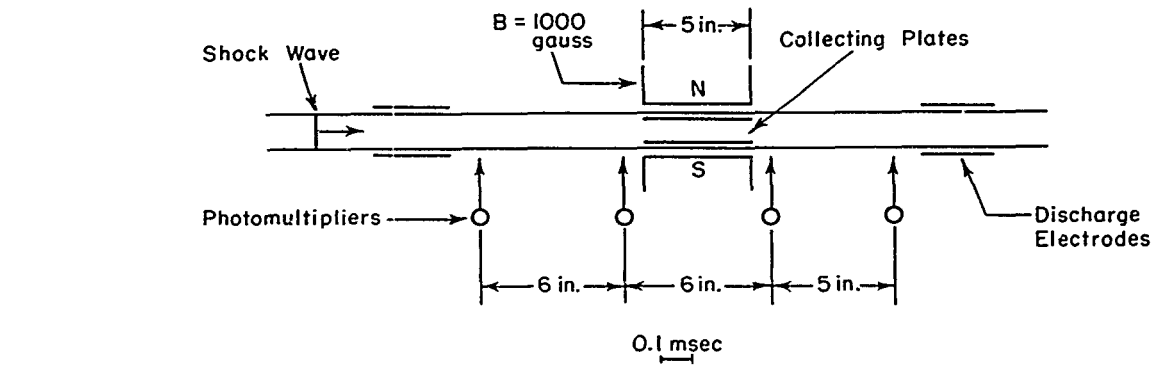

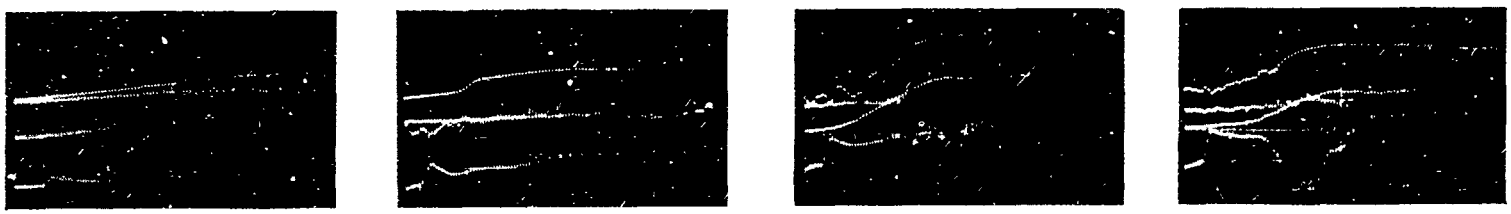

a. *b.* *c.* *d.*

P_1 (mm Hg)	0.91	1.01	0.61	0.50
W_{11}	2.46	2.48	2.61	2.66
I_d (ma)	210	184	205	200
Magnets Present	No	Yes	Yes	Yes
Collecting plate connections	Externally shorted	Open	Open	Externally shorted

Figure 11 Photomultiplier signals for measuring shock wave attenuation.
Each trace indicates discharge radiation viewed by separate photomultipliers.

0.1, 0.3, 0.5, and 0.68 msec. Careful inspection will reveal the breaks in the remaining frames; note that the relative position of the four traces is not the same in all frames.

Three different experimental arrangements are represented in Fig. 11, depending on whether the magnetic field was present or absent and on whether the collecting plates were shorted or open-circuited.

A detailed discussion of the results of this type of experiment is given in conjunction with Tables 3 and 5. Suffice it to say here that in successive experiments the shock speed was definitely lower in the presence of a magnetic field than with no magnetic field present; however, the shock attenuation observed within a given experiment could not be correlated with the changes that were made in experimental conditions.

THIS PAGE LEFT BLANK PURPOSELY.

5. DISCUSSION OF DATA

5.1 Some General Results

The electrical conductivity of the experimental gas was estimated from measurements of the impedance of the discharge. Although an effort was made to develop a conductivity detector[17], the development was terminated when it became evident that too large a fraction of the total effort would be required for its completion. The voltage across the discharge electrodes was measured with an rf voltmeter, with the aid of a capacitative voltage divider, and also with an oscilloscope using an attenuating probe. The load current was measured with a thermocouple ammeter and also by displaying on an oscilloscope the potential across a small known resistor in series with the load. Meter and oscilloscope measurements of both current and voltage were found to agree within about ten percent. One form of equivalent load impedance that was assumed consisted of a discharge resistance R, in series with two electrode capacitances C_e. From typical voltage and current measurements (V_d = 2860 v and I_d = 240 ma) and taking into account the measured lag (60 electrical degrees) of voltage behind current, the calculated values of R and C_e were 6000 ohms and 50 μμf, respectively. The electrode capacitance had been found to have the somewhat higher value of 70 μμf from Q-meter measurements in which the discharge was simulated by an aluminum rod. The power dissipated in the resistance was on the order of 200 watts; and the total power was 2900 watts, which is close to the rated 3 kw output of the induction generator used as a source of rf power.

If we picture the resistive component of the discharge as equivalent to a cylindrical resistor of length ℓ and cross-sectional area A, the conductivity can be calculated by the formula

$$R = \frac{\ell}{\sigma_o A} \qquad (15)$$

For A we used 5 cm^2, the cross-sectional area of the shock tube; and for ℓ we used the typical value of 100 cm. Taking R = 6000 ohms, we found the conductivity σ_o to be on the order of 1/3 mho/m.

We had expected, on the basis of literature examined before initiating this study, (see, for example, Reference 22) that a conductivity on the order of 1000 mhos/m could be achieved. Probably, the primary reason for the low values actually obtained is that the nature of the measurements we wished to make restricted our electrode arrangement to the type which yields an electrostatic discharge instead of the much more intense induced discharge of electromagnetic origin.

It is possible that the conductivity of the ionized gas was actually higher than the value estimated on the basis of impedance measurements. There exists a high resistance at the surface of electrodes in contact with an ionized gas and the resistance of the gas itself may actually be much smaller than the measured resistance. (See, for example, Reference 4, page 245.) Even allowing for this, however, it is not likely that the conductivity was greater than 10 mho/m in our experiments.

In order to calculate typical values of some other pertinent parameters we may consider a typical experiment, with argon in both sections of the shock tube. With an initial pressure of 1 mm Hg in the discharge section and a pressure ratio (P_{41}) of 300 across the diaphragm we would have, in the absence of any MHD interactions:

Mach number of incident shock wave: $W_{11} = 2.5$
Pressure behind incident shock wave: $p_2 = 7.5$ mm Hg
Gas velocity behind incident shock wave: $u_2 = 500$ m/sec
Gas density behind incident shock wave: $\rho_2 = 2 \times 10^{-3}$ kg/m^3

Using another expression for the conductivity

$$\sigma_o = \frac{n_e e^2 \tau}{m} \qquad (16)$$

where n_e = number of free electrons per unit volume

e = electron charge

m = electron mass

τ = mean time between successive collisions of electrons with neutral atoms

we can estimate the degree of ionization in our gas discharges. The value of τ was estimated to be 5×10^{-11} sec by dividing the mean electron velocity into the mean free path of electrons for collisions with neutral atoms. The electron velocity was estimated as 6×10^{8} cm/sec by assuming the mean kinetic energy of electrons to be on the order of the ionization energy, 10 ev; and the mean free path, calculated by standard techniques,[19] was found to be about 0.03 cm. The density of atoms was assumed to be that appropriate to the region behind the incident shock wave, or approximately 10^{17} atoms/cm^3. Equation 16 yields $n_e = 10^{11}$ electrons/cm^3 if we take $\sigma_o \sim 1$mho/m. Thus, only one out of a million argon atoms was ionized in the region behind the shock wave.

Chandrasekhar[18] derives the equations of motion for electrons in a fully ionized gas and in a partially ionized gas, in the presence of electric and magnetic fields, and shows how the value of σ_o, the conductivity in the absence of a magnetic field, is modified in these two situations. A comparison of the numerical coefficients of corresponding terms in the two equations of motion, for the conditions holding in our experiment, showed that, in spite of the low degree of ionization, the equation for a fully ionized gas applies to our experiment almost exactly. This meant that we could use the following expression to calculate the value of conductivity in the direction transverse to the field lines:

$$\sigma = \frac{\sigma_o}{1 + \omega_e^2 \tau^2} \qquad (17)$$

where $\omega_e = \frac{eB}{m_e c}$ is the gyro frequency of the electrons; i.e. the

angular rate of revolution in the Larmor circle about the field lines. For a magnetic field of 1000 gauss, we found $\omega_e = 1.6 \times 10^{10}$ radians/sec and

$$\sigma = \frac{\sigma_0}{1 + 0.08} = 0.93\, \sigma_0$$

Thus it appears that reduction of transverse currents, such as induced by MHD interaction, will not be too severe. The value of conductivity along the field lines is the same as its value σ_0, in the absence of a magnetic field.

The interaction parameter Γ, (Eqn. 14, Section 3) was estimated as follows: It was assumed that σ and u could be considered approximately constant over the interaction (magnetic field) region of length L, so that

$$\Gamma = \sigma u B^2 L \qquad (18)$$

Our magnetic field strength was on the order of 1000 gauss (1/10 w/m^2), and the interaction distance was on the order of 30 cm. The gas velocity behind the incident shock wave was typically 500 m/sec. Thus, taking $\sigma_0 \sim 1$ mho/m, we have

$$\Gamma = 1.5\ n/m^2 = 15\ \text{dynes/cm}^2 = 1.5 \times 10^{-7}\ \text{atm}$$

We recall that Γ is the term which must be added to the right side of the momentum equation (Eqn. 12, Section 3) to account for the MHD interaction. We are interested, therefore, in knowing how its value compares to that of the other terms in the same equation. In particular we are interested in the ratio Γ/p_2, where p_2 is the pressure behind the shock wave. In a typical experiment p_2 was 7.5 mm Hg, or on the order of 10^{-2} atm. Thus, Γ/p_2 is of order 10^{-5}.

There is a closely allied parameter, described by some as the ratio of "electric body force" to the dynamic force, which is equivalent to the ratio of Γ to the dynamic pressure

$$N = \frac{\text{electromagnetic force}}{\text{dynamic force}} = \frac{2\sigma B^2 L}{\rho u} = \frac{\Gamma}{\rho u^2/2} \qquad (19)$$

This parameter had a value of about 3×10^{-5} in a typical experiment. That Γ/p_2 and N should be of the same order is not surprising in view of the fact that the static and dynamic pressures are comparable in magnitude. These parameters (Γ/p_2 and N) should be at least comparable to unity in order for the free stream conditions to be modified by the MHD interaction. Because they were found to be so small we did not expect to detect any MHD effects. It happened, however, that appreciable shock wave attenuations were observed under conditions that led us to believe an MHD interaction was responsible, though perhaps of different origin from the expected one.

Another important parameter is the magnetic Reynolds number

$$R_m = \mu\sigma u L \qquad (20)$$

This parameter can be interpreted as the ratio of the magnetic field due to induced currents, to the applied magnetic field. The induced field is μ times the integral of the current density, $\sigma\vec{v} \times \vec{B}$, over a distance of the order of L, yielding a quantity of order $\mu\sigma uBL$, where L is the extent of the magnetic field in the direction of motion. Dividing by the applied field yields Expression 20. In our experiment, with $\mu \approx \mu_o = 1.257 \times 10^{-6}$ kg m/coul^2, and the other variables given the same values as above, we find $R_m \sim 2 \times 10^{-4}$. Thus, the induced field could be regarded as a negligible perturbation of the applied field.

5.2 Shock Wave Attenuation Data.

The experimental data are summarized in Tables 1 to 5, accompanying each of which there is a discussion of the experimental arrangements and the significance of the observations. In most instances the data were subjected to statistical analysis in order that the effects of various changes in experimental conditions might be established with known confidence. As many of the experiments were exploratory in nature they were not planned with a statistical analysis in view. Often, the achievement of a particular objective required that each successive experiment in a series be modified according to the findings of the preceding experiments. This fact hampered the analysis in a few cases. Details of the statistical techniques applied are discussed in Appendix B.

The data listed in Table 1 were obtained with the arrangement indicated at the upper left of Fig. 8. Both the driver gas and the experimental gas were air. The Table lists the initial pressure of the experimental gas and the discharge current prior to propagation of a shock wave through the ionized air. The Mach number of the shock wave was approximately 2.5 in all experiments. There are five groups of experiments which differ according to whether a magnetic field was present and whether a screen was placed inside the shock tube. The "screen" was actually a tube, formed from bronze fly screening, made to fit snugly inside the glass section of the shock tube. It was located, when used, between the two shock wave detectors, coinciding with the location of the magnetic field when it was present. The purpose of the screen tube was to provide a path in which transverse currents that might be produced by an MHD interaction could flow.

The time t', taken by the shock wave to travel from the upstream to the downstream photomultiplier detector was measured as described in conjunction with Fig. 9. The corresponding theoretical

Table 1 Summary of Shock Speed Experiments with Air

Group	Magnets	10 in. Screen	Exp.No.	I_d	P_1	$\frac{100\ \Delta t}{t}$	95% Confidence Limits
				(ma)	(mm Hg)	(%)	
a			55	90	0.58	-4.6	
			57	62	1.0	-2.6	
			59	85	0.5	2.5	
			61	92	0.72	5.3	
			62	95	0.72	-3.0	
			Average	85		-0.48	± 5.7
			Std.Dev.			4.2	
b	x		63	58	0.55	1.1	
			64	65	0.54	-2.4	
			65	65	0.50	-6.9	
			70	57	0.57	7.1	
			82	60	0.57	16	
			83	62	0.49	14	
			Average	61		4.8	± 5.2
			Std.Dev.			9.2	
c	x*		74	65	0.43	19	
			75	65	0.39	23	
			76	65	0.51	18	
			Average	65		20	± 7.4
			Std.Dev.			2.6	
d		x	77	90	0.53	23	
			78	90	0.52	22	
			Average	90		22.5	± 9.0
			Std.Dev.			0.7	
e	x	x	66	75	0.51	24	
			67	75	0.33	24	
			79	80	0.65	28	
			80	80	0.57	31	
			Average	78		26.8	± 6.4
			Std.Dev.			3.4	

* Five permanent magnets set so fields of adjacent magnets were oppositely directed.

time, t, was calculated from the initial ratio of pressures across the diaphragm, on the basis of the usual one-dimensional shock tube theory. In these calculations the properties of the experimental gas were assumed to be unaffected by establishment of the rf discharge. This assumption seems justified in view of the small amount of power dissipated within the gas by the discharge; theoretical estimates of pressure and temperature changes produced by the discharge were negligibly small.

The quantity $\frac{100\Delta t}{t}$, for which we shall use the abbreviation α, and in which $\Delta t = (t' - t)$, is the percent by which the measured time exceeds the theoretical time. It is a measure of the extent to which the shock wave is attenuated with respect to its theoretical speed. The average and standard deviation of this quantity are listed for each group of experiments. The 95% confidence limits as calculated in the Appendix are also listed.

The time t' was measured with an accuracy of approximately $\pm$ 3%. If we assume that t, which was approximately 500 μsec in all the experiments of Table 1, was calculated exactly, it follows that the accuracy of α is the same as the accuracy of Δt. In Group a, t' was measured to within $\pm$ 15 μsec; but t' was only 2.5 μsec on the average. Hence, the measurement error in Δt and α was about $\pm$ 600% in Group a. Similarly, we find that Group h, with a larger Δt, has a correspondingly smaller measurement error, of $\pm$ 15%.

The statistical analysis described more fully in Appendix B showed that, with considerable confidence, the data in the various groups could be regarded as having equal variability. An analysis of variance showed that differences among the means of the five groups could not have occurred by chance alone. A "gap and straggler" analysis applied to the groups, ordered according to means, showed the following: The mean value of α in Group c is significantly greater than the mean value in Group b, which is itself significantly greater than the mean value in Group a. There is no significant

difference between Groups c and d. A 95% confidence level was chosen as a basis for the above statements. We can regard the difference between Groups d and e as significant only with a lower level of confidence, below 90%.

We may now consider the correlation between the average values of α and the experimental conditions. Primarily because of low electrical conductivity in the working gas, MHD effects were expected, theoretically, to be negligible. Many of the observed shock wave attenuations could not be explained, however, except as effects of an MHD interaction whose magnitude exceeded the theoretical prediction. In Group a, with neither magnets nor screen present, there is no reason to expect the measured and calculated shock travel times to differ. (Shock waves are known to decelerate in travelling along a tube, but at low Mach numbers and in short tubes this effect is small.) Indeed, α is close to zero for Group a; the fact that the average value is slightly negative is of no concern in view of the large measurement error in this group. In Group b, with a magnetic field present, but with no path provided for induced currents, an MHD interaction might be expected to take place only at the edges of the magnetic field, where a gradient exists. That some shock attenuation occurred is evidenced by the fact that α_b was significantly greater than α_a. In Group c, the five magnets used in arrangement b were realigned so that adjacent magnets were oppositely directed. With six regions of field gradient, instead of two, one might expect an attenuation on the order of three times that in Group b; the observed average attenuation is actually about four times as great. The factor four has little meaning; for, on the basis of statistical analysis we can say only that the attenuation was significantly greater in Group b than in Group a. In Group d we determined the shock attenuation caused by the tubular screen in the absence of any MHD effect. There is no basis for comparing the value of α in Group d with its value in the preceding

groups, except that it should be greater than the value in Group a, which is certainly true. Finally, in Group e, with both magnetic field and screen present, we might expect α to exceed its values in Groups b and d. Again we find the observation to agree with our expectation, provided we accept a lower confidence level for the assertion $\alpha_e > \alpha_d$.

The data in Table 2 were obtained in experiments which differ from those in Table 1 only in that air was replaced by argon and the collecting plates previously described had been installed in the shock tube. The arrangement was that shown in Fig. 10. The measurement error was approximately the same as in Table 1. However, the same analysis as was applied to Table 1 showed that the argon experiments could not be regarded as having equal variability. Because of this a more complex analysis of variance was required, but again the result showed that the differences among the means of the various groups could definitely not all be regarded as having occurred by chance. The groups were again ordered according to the value of the mean and the significance of differences in successive means was analyzed. According to this analysis only Groups k and l, among all successive pairs, were found to be significantly different; the mean value of α in Group l being significantly greater than the mean value in Group k. The lack of significant difference between the remaining successive pairs does not imply that there is no significant difference between non-successive pairs of groups. In view of the difficulty of further analysis it was decided to judge the differences between non-successive pairs of experimental groups as objectively as possible without resorting to an elaborate statistical examination. A discussion of the correlation between observed shock attenuation and experimental conditions for data in Table 2 is given below, following the introduction of Fig. 12 and Table 4, where it is more convenient to do so.

Table 2 Summary of Shock Speed Experiments with Argon

Group	Magnets	10 in. Screen	5 in. Copper Plates	Exp.No.	I_d (ma)	P_1 (mm Hg)	$\frac{100\,\Delta t}{t}$ (%)	95% Confidence Limits
f	x		x	108	145	0.83	1.7	
				109	155	0.60	3.6	
				111	177	0.77	0.23	
				114	195	0.57	8.8	
				122	165	0.75	9.8	
				Average	167		4.8	± 5.3
				Std.Dev.			4.3	
g			x	106	220	0.77	9.2	
				107	180	0.93	-2.4	
				135	220	0.64	8.8	
				136	225	0.77	9.3	
				Average	211		6.2	± 9.0
				Std.Dev.			5.8	
h	x		x**	112	200	0.64	9.0	
				113	190	0.71	9.5	
				123	165	0.80	8.5	
				Average	185		9.0	± 1.2
				Std.Dev.			0.5	
i			x*	130	225	0.79	22	
				131	230	0.74	9.3	
				132	217	0.82	7.1	
				133	225	0.80	13	
				134	222	0.94	9.6	
				Average	224		12.2	± 7.3
				Std.Dev.			5.9	
j	x		x*	124	165	0.68	14	
				125	170	0.68	14	
				126	180	0.72	16	
				128	150	0.88	8.2	
				129	165	0.61	16	
				Average	166		13.6	± 4.0
				Std.Dev.			3.2	
k		x	x	116	230	1.05	17	
				117	250	0.93	15	
				118	235	0.63	13	
				119	245	0.69	18	
				Average	240		15.8	± 3.5
				Std.Dev.			2.2	
l	x	x	x	115	—	0.81	20	
				120	190	0.78	20	
				121	197	0.80	21	
				Average	194		20.3	± 1.4
				Std.Dev.			0.6	

* Plates shorted by copper cylinder, 1-1/4 in. long, inside shock tube.

** Plates shorted with external clip lead.

The data listed in Table 3 were obtained with the experimental arrangement shown in Fig. 11, four photomultipliers being used to measure the shock speed in three regions: the interaction (magnetic field) region and regions upstream, and downstream of the interaction region. In Table 3, use is made of only that part of the data which apply to the interaction region. Except for the fact that the subscript "23" is used to refer to this region, the quantities t, t', Δt and α ($= \frac{100\Delta t}{t}$) have the same meaning as in Tables 1 and 2. Argon was used in both the driver and experimental sections of the shock tube. The four groups of experiments differ according to whether a magnetic field was present and whether the collecting plates were open-circuited or externally shorted with a clip lead.

A statistical analysis of these data was performed, as described in Appendix B, by expressing the mean value of α as the sum of four terms: the first term was the mean value of α for the condition of open circuit and no magnetic field; the second term represented the effect, on the mean value of α, produced by the magnetic field; the third term represented the effect of short-circuiting the collecting plates; and the fourth term represented the simultaneous effect of magnetic field and short-circuiting. Evaluation of the four terms by the method of least squares showed that only the magnetic effect was clearly significant. The other effects might be significant, but the data do not allow a definite conclusion. Because of the greater difficulty in measuring travel time on the oscilloscope records, such as shown in Fig. 11, the data in these experiments had somewhat greater measurement errors than the data in Tables 1 and 2. As was done with Table 2, a discussion of the correlation between observed shock wave attenuations and experimental conditions is postponed until Fig. 12 and Table 4 are introduced.

Table 3 Shock Speed Data Obtained with Collecting Plate Arrangement.

Group	Magnets	Collecting Plates	Exp.No.	I_d (ma)	P_1 (mm Hg)	W_{11}	t_{23} (μsec)	t'_{23} (μsec)	Δt_{23} (μsec)	$\frac{100\,\Delta t_{23}}{t_{23}}$ (%)	95% Confidence Limits
m	Absent	Open circuited	154	223	1.00	2.45	190.4	203	13	6.4	
			155	225	1.07	2.43	192	205	13	6.3	
			156	227	0.65	2.58	181	203	22	10.8	
			157	225	0.78	2.49	187	212	25	11.8	
			Average	(225)						(8.8)	± 3.1
n	Absent	Short circuited	158	213	0.95	2.46	190	205	15	7.3	
			159	210	0.86	2.48	188	210	22	10.5	
			160	210	0.91	2.46	190	207	17	8.2	
			161	232	1.08	2.42	193	211	18	8.5	
			Average	(216)						(8.6)	± 3.1
o	Present	Open circuited	165	180	0.90	2.49	232	280	48	17.2	
			167	186	0.92	2.49	240	262	22	8.4	
			169	184	1.01	2.48	263	302	39	12.9	
			170	183	0.79	2.56	282	310	28	9.0	
			171	168	0.50	2.63	226	263	37	14.1	
			172	200	0.60	2.59	232	262	30	11.4	
			173	205	0.51	2.63	229	257	28	10.9	
			174	205	0.61	2.61	230	254	24	9.5	
			175	195	0.34	2.72	220	251	31	12.4	
			176	195	0.50	2.63	228	247	19	7.7	
			177	200	0.41	2.70	222	265	43	16.2	
			178	195	0.56	2.63	228	283	55	19.4	
			Average	(190)						(12.4)	± 1.8
p	Present	Short circuited	179	200	0.50	2.66	226	255	29	11.4	
			180	195	0.54	2.63	228	257	29	11.3	
			181	200	0.54	2.63	228	273	45	16.5	
			182	180	0.41	2.68	224	254	30	11.8	
			183	195	0.37	2.72	220	249	29	11.6	
			184	190	0.44	2.71	221	250	29	11.6	
			185	190	0.39	2.74	219	250	31	12.4	
			Average	(193)						(12.4)	± 1.8

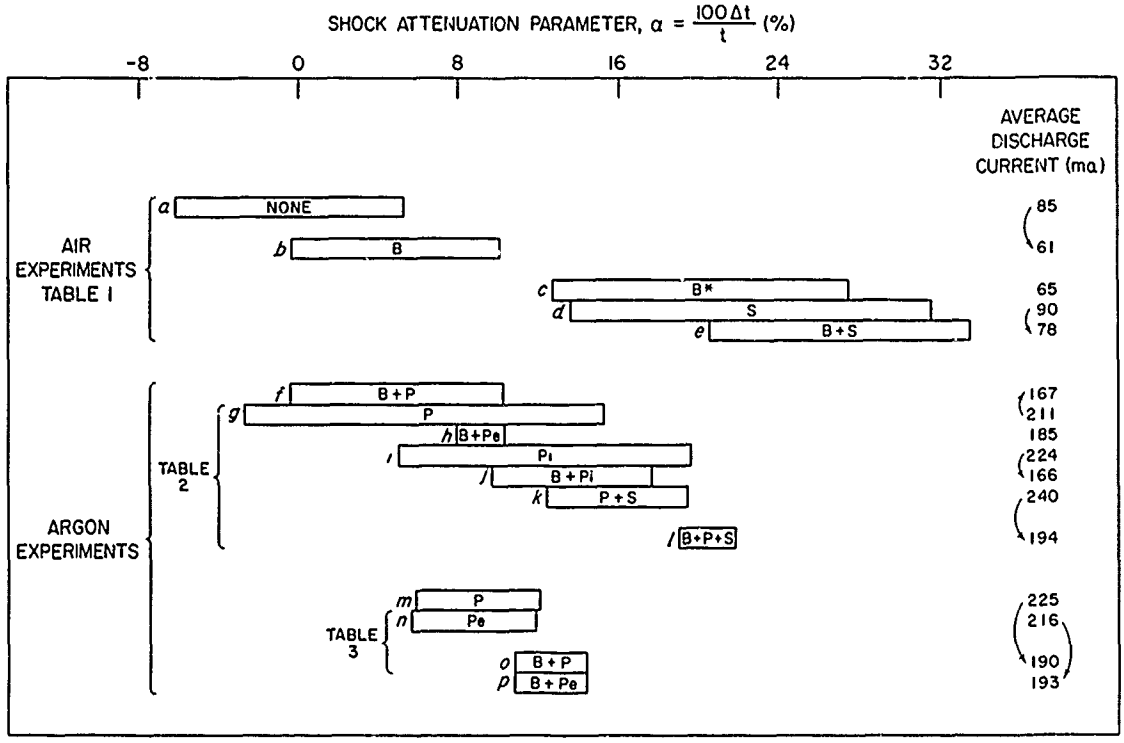

Figure 12. Summary of Tables 1, 2, and 3.

The ends of each bar coincide with the 95% confidence limits of α.
Average discharge current in milliamps is given at right for each bar (see text for meaning of arrows).
Statistically, there is no significant difference in α for any pair of successive bars which are drawn touching one another.
Small letters to the left of the bars correspond to the group designations given in the Tables.
Capital letters within the bars indicate the experimental arrangement:

B	Transverse magnetic field of 1000 gauss provided by permanent magnets. For Tables 1 and 2, field region was 20 cm long. For Table 3, field region was 12 cm long.
B^*	Five magnets set so adjacent ones were oppositely aligned.
P	Collecting plates present.
P_e	Collecting plates shorted externally with clip lead.
P_i	Collecting plates shorted internally with short copper tube.
S	Ten inch long tube of bronze fly screen present.

The data presented in Tables 1 to 3 have been summarized in Figure 12. The horizontal scale represents the value of α, and for each group a horizontal bar has been drawn with its ends at the 95% confidence limits. The vertical order of groups within each set corresponds to the order of the mean values of α. Furthermore, successive bars are spaced apart in the vertical direction only if the statistical analysis showed the corresponding groups to be significantly different. The experimental arrangements are indicated by letters within each bar. Thus, one can tell by a glance at the figure what was observed to be the effect of various changes in experimental conditions on the attenuation of the incident shock wave.

It is interesting to consider the agreement between the results summarized in Fig. 12, and the relevant theory. As far as magnetohydrodynamic effects are concerned, we have indicated that — particularly because of the small electrical conductivity achieved — such effects were expected theoretically to be negligibly small. However, appreciable shock wave attenuations were observed in our early experiments. Careful consideration of the individual processes occurring in the experiment yielded several speculations but no satisfactory explanation of the apparent disagreement with theory. Therefore, it seemed useful to conduct further experiments to establish the cause of the observed attenuations. In comparing the results to be expected for different experimental arrangements there were two general situations encountered. One situation involved arrangements which differed only "mechanically"; i.e., the difference had no relevance to MHD theory. In such situations it was nevertheless useful to compare observations with qualitative predictions of the relative shock attenuations because of its bearing on the general reliability of the experiments. The other type of situation involved differences in experimental arrangement which might conceivably affect the MHD interaction, except for the fact that all such interactions

Table 4 Agreement of Shock Attenuation with Theory

Relative Size of Shock Attenuation Parameter, in Various Experimental Groups		Inequality Agrees with MHD Theory	Inequality Agrees with Theory not Bearing on MHD
Based on Statistical Analysis	Based on Analysis Aided by Informal Reasoning		
Table 1			
b>a		x	
c>b		x	
d>a, b			x
e>d*		x	
Table 2			
l>k		x	
	h>f	x	
	j>f		x
	k>g		x
	i>g		x
	j>h		x
Table 3			
	(o≈p)**	x**	
o>m, n		x	

* The confidence level for this assertion is somewhat less than 90%, whereas it is 95% in all other cases.

** Groups o and p had identical confidence limits, and the difference between these limits was smaller than in any other group, except one. We considered it appropriate, therefore, to assert that the shock attenuation was approximately the same in Groups o and p. This assertion agrees with the theoretical prediction that Groups o and p should be neglibibly different. As described in the text, this assertion was not completely consistent with the others.

were theoretically negligible in our experiments. Allowing for the possibility that the true interaction might be stronger than predicted, it seemed useful in these situations at least to compare the observed attenuations with the "qualitative" prediction concerning their relative values. As will be shown below none of the possible comparisons, under both types of situations, resulted in a contradiction of the theory.

The agreement of the observed shock attenuation with theory is represented in Table 4. The two left hand columns include all the instructive assertions that could be made concerning the relative shock attenuation in the various groups of experiments. The expression b>a, for example, is an abbreviation for the statement, "The average shock attenuation in experiments of Group b is significantly greater than the average shock attenuation in experiments of Group a." Expressions in the first column were based on the statistical analysis described in Appendix B, but those in the second column required the aid of less formal considerations as well. For example, the inequality h>f was not proved by statistical analysis; however, a comparison of the ranges of α for Groups h and f in Fig. 12 with the ranges of α in other pairs of experimental groups, such as a and b, which were shown to be unequal mathematically, indicates that the assertion h>f can be made with considerable confidence. As shown in the third and fourth columns of Table 4, all the inequalities are in the direction expected either on the basis of MHD theory, or of theory not involving MHD, whichever was applicable. A discussion of the physical basis for asserting that the inequalities in Table 4 agree with theory is given in Subsection 5.3. The assertion of the approximate equality of Groups o and p agrees with the theoretical expectation that Group p should be negligibly greater than Group o; but it is not altogether consistent with the remaining assertions in Table 4, where pairs of groups to which a similar theoretical prediction applied were found

to be significantly different, with the inequality in the expected direction.

With one exception, therefore, a general result of our analysis of the shock wave attenuation data is that, wherever the data permitted a clear distinction between any two sets of experimental conditions, the observed inequality of shock attenuation was always in the expected direction but, when the situation involved MHD theory, the magnitude of the difference was much greater than predicted.

Before leaving our discussion of Fig. 12 and Table 4, we will examine the possible influence of the magnitude of the discharge current on the shock wave attenuation.

In Fig. 12, the average discharge current for each group of experiments is listed in a column to the right. The numbers in this column show, for one thing, that the discharge current was considerably greater with argon than with air as the experimental gas. This is associated with the fact that a monatomic gas such as argon is more easily ionized than air, in which the electrons use a large part of the energy they gain from the field in exciting the vibrational levels of the molecules and in dissociating them. Further inspection of the discharge currents reveals an interesting feature: if we choose those pairs of experiments whose arrangement is identical, except for the presence or absence of a magnetic field, we find that the discharge current was invariably smaller in the presence of a magnetic field. This, in itself, is not surprising. We found evidence that the permanent magnets had a tendency to shunt some of the rf power so that less power was dissipated within the ionized gas. Of more interest is the fact that the shock wave attenuation was greater whenever the magnetic field was present, except in one case which was among those that indicated no significant change on a statistical basis. One might ask therefore whether the shock wave attenuation ought to be correlated with the change in discharge current instead of the magnetic field. An argument against such a suggestion is the

fact that lower discharge current is probably associated with lower gas conductivity and therefore with a smaller, instead of a greater, MHD effect. It seems more reasonable to conclude that the MHD effect occurred in spite of the reduction in conductivity brought about by introducing the magnetic field.

The data in Table 5, like that in Table 3, was obtained with the experimental arrangement shown in Fig. 11. The quantities V_{12}, V_{23}, and V_{34} represent the measured shock speed in three continuous displacements along the shock tube. The subscript "23" refers to the interaction region, and subscripts "12" and "34" refer to regions upstream and downstream, respectively, of the interaction region. The gas used in driver and experimental sections of the shock tube was argon. In all experiments a magnetic field of approximately 1000 gauss was present in the interaction region. The only difference between the two groups of experiments was that the collecting plates were open in the first group and shorted by a clip lead in the second group.

As mentioned in conjunction with Fig. 10, this arrangement represents an attempt to detect an MHD effect within a given experiment; it was hoped that an examination of the changes in velocity from region to region would make this possible.

The differences in velocities in successive regions, $(V_{12} - V_{23})$ and $(V_{23} - V_{34})$, are subject to considerable error. The time measurement is subject to an error of $\pm$ 5% and the distance measurement to an error of at least $\pm$ 1%. Hence, the error of an individual velocity is at least $\pm$ 6%. The velocity differences, of approximately 1 $^{in}/_{sec}$, are thus subject to an error of $\pm$ 2 x 1.8 $^{in}/_{sec}$ (2 times 6% of 30 $^{in}/_{sec}$) or approximately $\pm$ 360%. Even if we assume that the time error is completely eliminated in taking an average, we are still left with an error of $\pm$ 2 x 0.3, or $\pm$ 60%, in the average values of velocity differences. It is clear, therefore, that with such large measurement errors in the mean values of the two velocity

Table 5 Shock Wave Deceleration Data.

Collecting Plate Arrangement	Exp.No.	V_{12}	V_{23}	V_{34}	$(V_{12}-V_{23})$	$(V_{23}-V_{34})$
		(in/sec)				
Open Circuited	171	30.0	28.7	28.9	1.3	-0.2
	172	31.0	29.2	28.7	0.8	0.5
	173	30.9	29.8	28.8	1.1	1.0
	174	30.4	30.1	28.2	0.3	1.9
	175	31.5	30.4	28.3	1.1	2.1
	176	30.5	29.9	28.0	0.6	1.9
	177	30.7	28.8	27.5	1.9	1.3
	178	29.6	29.2	27.6	0.4	1.6
	Average				(0.94)	(1.26)
Short Circuited	179	31.3	29.9	28.0	1.4	1.9
	180	31.9	30.2	28.2	1.7	2.0
	181	27.4	27.8	26.9	-0.4	0.9
	182	31.8	30.1	28.9	1.7	1.2
	183	33.0	30.6	30.0	2.4	0.6
	184	32.0	30.5	30.8	1.5	-0.3
	185	30.3	30.5	30.6	-0.2	-0.1
	Average				(1.16)	(0.89)

changes, $(V_{12} - V_{23})$ and $(V_{23} - V_{34})$, it is impossible to draw any conclusions pertaining to their relative values. The experiments would have been successful only if the velocity changes had turned out to be considerably greater.

In addition to demonstrating the need for greater accuracy, these experiments were useful in providing data for Table 3, which showed, essentially by a comparison of the measured V_{23} with its theoretical value, that the magnetic field caused a significant increase in the shock wave attenuation.

The data reported in Table 5 represent the end of our experimental effort as of the writing of this report.

5.3 Physical Basis for Inequalities in Table 4.

This section considers the physical basis for claiming that the inequalities (and one equality) listed in Table 4 are in agreement with theoretical expectation. The inequalities concerning Groups from Table 1, which were discussed in Subsection 5.2, are omitted from the following discussion to avoid repetition.

$l > k$ These two groups are essentially a repetition, with argon instead of air, of Groups d and e, respectively, given in Table 1; the presence of the collecting plates, which had been installed in the meantime, is the only other experimental difference. Again, the object was to see whether a magnetic field would increase the shock attenuation. In the argon experiments we observe that the difference between the two groups of experiments is in the direction expected; it is somewhat greater than in the air experiments; and finally, statistical analysis shows the difference to be significant with a high level of confidence. This is a situation, then, in which the observed inequality was in the direction expected, but was much greater than predicted theoretically.

$h > f$ These two groups were intended to demonstrate the effect of having the collecting plates open-circuited or shorted;

shock attenuation was expected to be greater in the latter case (Group h) in which induced currents, if present and capable of reaching the plates, would have a closed flow path available. The average attenuation observed in Group h is seen to be approximately twice that observed in Group f. Again the difference is in the appropriate direction, but much greater than expected.

j > f The comparison of these two groups parallels the comparison above of Groups f and h. The only difference is that the plates were shorted internally in Group j instead of externally as in Group h. There appears to be an additional attenuation contributed by the internal shorting cylinder itself, as discussed more fully in the discussion of the assertion j > h.

k > g It is useful to compare these two groups of experiments only to the extent that their satisfactory outcome lends support to the validity of the data. It might be expected that the flow resistance offered by plates and screen would be greater than the resistance of plates alone; and this seems to be borne out by the greater shock attenuation observed in Group k.

i > g This comparison parallels that of Groups g and k. Again we observed that an additional flow resistance, that offered by the internal shorting cylinder, contributed to increased shock attenuation. In addition, the difference between these two groups helped to allow for the frictional effect of the shorting cylinder in the comparison of Groups f and j, and Groups h and j.

j > h These two groups, just as those in the above paragraph, differed only by the presence of the internal shorting cylinder in Group j. The shock attenuation in Group j might be expected to exceed that in Group h not only because of the flow resistance offered by the shorting cylinder but also because it effectively increased the length of the interaction region; the latter effect is theoretically negligible, however. The observed attenuation in these two groups agrees qualitatively with this expectation.

$o \approx p$ Groups o and p involved an arrangement in which collecting plates and the magnetic field were present; the only difference between the two groups was that the plates were externally short circuited with a clip lead in Group p. As in the comparison of Groups f and h, from Table 2, the theoretical prediction is that shock attenuation will be greater in Group p, but by a negligibly small amount. The data in this case indicate that, if there is a difference between α_o and α_p, the difference is likely to be small, and either α_o or α_p can be expected to have the greater value. The fact that an appreciable difference between α_o and α_p is unlikely agrees with the negligible effect predicted theoretically.

$o > m, n$ Because of MHD interaction in the gradient regions at the ends of the magnetic field region, theory would predict greater shock wave attenuation (by a negligibly small amount) in Group o than in Groups m or n, which had no magnetic field. Again, the difference was in the direction expected, but of greater magnitude than predicted by theory.

CONCLUSION

We have seen that statistical analysis of the data permits us to associate shock wave attenuation by MHD interaction with the following experimental factors: interaction within a region of magnetic field gradient in the absence of electrodes for collecting induced currents and interaction in a region of uniform magnetic field with collecting electrodes provided. The electrode arrangements which appeared to contribute to an MHD interaction included a cylindrical screen and parallel plates shorted either internally (by being in contact with the tubular screen) or externally with a clip lead, in the absence of the tubular screen. There was one case, however, in which externally shorted plates appeared to have little, if any, effect.

In summary, we can say that wherever changes in experimental conditions led to significant changes in shock wave attenuation the direction of the changes agreed with those expected theoretically, but the magnitude of the changes greatly exceeded the negligible effects predicted.

It is interesting to note that other workers have also, in some similar experiments, observed greater effects than expected. In a steady flow experiment,[20] for example, in which an rf field was applied to plates inside a glass tube and induced currents were collected by the same plates, it was found that their magnitude was much greater than predicted theoretically. In another experiment,[21] involving the detection of the Hall voltage in a gas ionized by rf power, voltages as much as 20,000 times higher than expected were observed. The hypothesis that they offer as the most reasonable explanation was that lack of symmetry in the probes and their arrangement caused the ionization level and charge distribution to be so altered, in the presence of rf power, that the observed voltage was generated.

The apparent discrepancies between theory and experiment remain unexplained. Since the real conditions existing within the interaction region are considerably more complex than the simple descriptions provided in the theoretical models it is possible that we have taken account of the real conditions inadequately, either through oversimplification, or through lack of awareness of an essential phenomenon. From careful consideration of the experimental procedure and the data it is not considered likely that the observations can be explained on the basis of a trivial factor that was overlooked. We have formed some speculations, of which an example is given below, but no satisfactory picture has been worked out.

Of the various explanations of our findings that we have considered, the one which seems most attractive involves the possibility that a boundary layer phenomenon results in a rectification of the rf ionizing field. This thought is based on the idea that the observed shock wave attenuations may be related to transverse currents whose magnitude exceeds that which would be contributed merely by the interaction of the conductive gas moving through the magnetic field. Rectification of the rf voltage was considered a possible source of appreciable transverse currents. Perhaps the influence of the electric body force on the sheaths adjacent to the collecting electrodes is unsymmetrical in such a way as to cause rectification. As discussed earlier in this report, attempts to detect rectification failed due to experimental difficulties; and we have, therefore, no experimental evidence either in favor of, or against the occurrence of rectification.

The apparent discrepancy between theory and experiment is thought to be worthy of further investigation. Instead of continuing

the study of gross phenomena it is considered that future work should lean toward the investigation of more detailed phenomena, such as the conditions existing within charged sheaths adjacent to electrode surfaces in the presence of electric and magnetic fields.

S. P. Carfagno
Senior Staff Physicist

G. P. Wachtell
Principal Scientist

Approved: F. L. Jackson
Assistant Director of Laboratories

REFERENCES

1. "Experiments in Magneto-Fluid Dynamics," R. A. Alpher; Physics Today, v 13, n 12, pp 26-31.

2. "Magnetohydrodynamics," T. G. Cowling; Interscience Publishers, Inc., New York; 1957.

3. "Magnetohydrodynamics in Aeronautics," W. R. Sears; paper 709-58 presented at American Rocket Society 13th Annual Meeting, November 1958.

4. "Prospects for Magneto-Aerodynamics," E. L. Resler, Jr. and W. R. Sears; Journal of the Aeronautical Sciences, v 25, pp 235-245, 258; April 1958.

5. "Plasma Physics," R. M. Kulsrud; American Scientist, v 48, n 4, p 581; December 1960.

6. "A Theoretical and Experimental Study of the Shock Tube," I. I. Glass, W. Martin, and G. N. Patterson; University of Toronto Institute of Aerophysics Report No. 2; November 1953.

7. "Elements of Gas dynamics," H. W. Liepmann and A. Roshko; John Wiley and Sons, Inc., New York, 1957.

8. "Electrical Conductivity of an Ionized Gas Produced by Strong Shock Waves," S. C. Lin, Thesis, Cornell University, 1952.

9. "Review of Recent Work on Strong Shock Waves Done at Cornell University," R. M. Patrick and A. Kantrowitz, Proceedings Aerothermochemistry Gas Dynamics Symposium; D. K. Fleming, Editor; Northwestern University, 1956; pp 255-263.

10. "One Dimensional Flow of an Ionized Gas through a Magnetic Field," R. M. Patrick and T. R. Brogan; Research Report 13, AVCO Research Laboratory, Everett 49, Massachusetts; October 1957.

11. "The Interaction of a Plane Strong Shock Wave with a Steady Magnetic Field," J. H. deLeeuw; University of Toronto Institute of Aerophysics Report No. 49; March 1958.

12. "The Design and Analysis of Industrial Experiments," edited by O. L. Davies; Hafner Publishing Company, New York; 1956.

13. "Statistical Analysis in Chemistry and the Chemical Industry," C. A. Bennett and N. L. Franklin; John Wiley and Sons, Inc., New York; 1954.

14. "Comparing Individual Means in the Analysis of Variance," J. W. Tukey; Biometrics, no. 2, vol 5; June 1949; pp 99-114.

15. Project Squid, Semi Annual Progress Report; April 1, 1959; pages 15 to 21.

16. Project Squid, Semi Annual Progress Report; October 1, 1959; pages 15 to 21.

17. Project Squid, Semi Annual Progress Report; April 1, 1960; pages 17 to 25.

18. "Plasma Physics," by S. Chandrasekhar; University of Chicago Press; 1960; Sections 53 and 54.

19. "Ionization and Breakdown in Gases," F. Llewellyn-Jones; John Wiley and Sons, Inc; New York; 1957; pp 17, 18.

20. "MHD Channel Flow"; D. E. Cunningham, R. G. Weirick, R. B. Block; Thompson Ramo-Wooldridge, Inc.; Paper presented at AIEE Symposium on the Engineering Aspects of Magnetohydrodynamics; February 1960.

21. "A Study of the Hall Effect in Gaseous Conductors"; by B. N. Edwards; Electronics Research Laboratory Scientific Report No. 6; University of California; Berkeley, California; September 30, 1959.

22. "Plasma Physics"; J. E. Drummond; McGraw-Hill Book Co.; 1961; Chapter 6.

APPENDIX

APPENDIX A. THEORY OF THE SIMPLE SHOCK TUBE

During the past fifteen years the shock tube and modifications of it have been used successfully for studying purely aerodynamic phenomena and for studying physical and chemical properties of gases at high temperature. Its theory and capabilities are well known from the extensive literature available. For this reason only a brief discussion of shock tube theory is presented here. Reference 6 was found to be very useful for acquiring a knowledge of shock tube theory and to learn about their construction and operation; it includes an extensive list of references to other pertinent literature.

A shock tube consists essentially of a long tube separated by a diaphragm into two parts, a driver section and an experimental section. Initially these two sections are filled with gas at rest, the pressure being higher in the driver than in the experimental section. In all our work the initial temperature in both sections has been room temperature. Heating due to establishment of an rf discharge in the low pressure section was assumed to be negligible. When the diaphragm shown in Figure 13a is suddenly ruptured a series of events occurs which can be followed by referring to Figure 13b. The theory of the shock tube assumes that the diaphragm disappears instantaneously, allowing the driver gas to expand into the experimental section. A contact surface, C, representing the boundary between the gases initially separated by the diaphragm, moves into the experimental section. This surface acts like a piston that has attained constant speed through instantaneous, infinite acceleration. This "piston" compresses the gas in front of it, quickly generating a shock wave, S, which advances at supersonic speed into the gas ahead of it. The shock front compresses the experimental gas to an intermediate pressure and accelerates the compressed gas toward the front. Simultaneously a rarefaction wave, R, is generated behind the "piston", and advances into the driver gas. The rarefaction wave expands the driver gas to the same intermediate pressure and

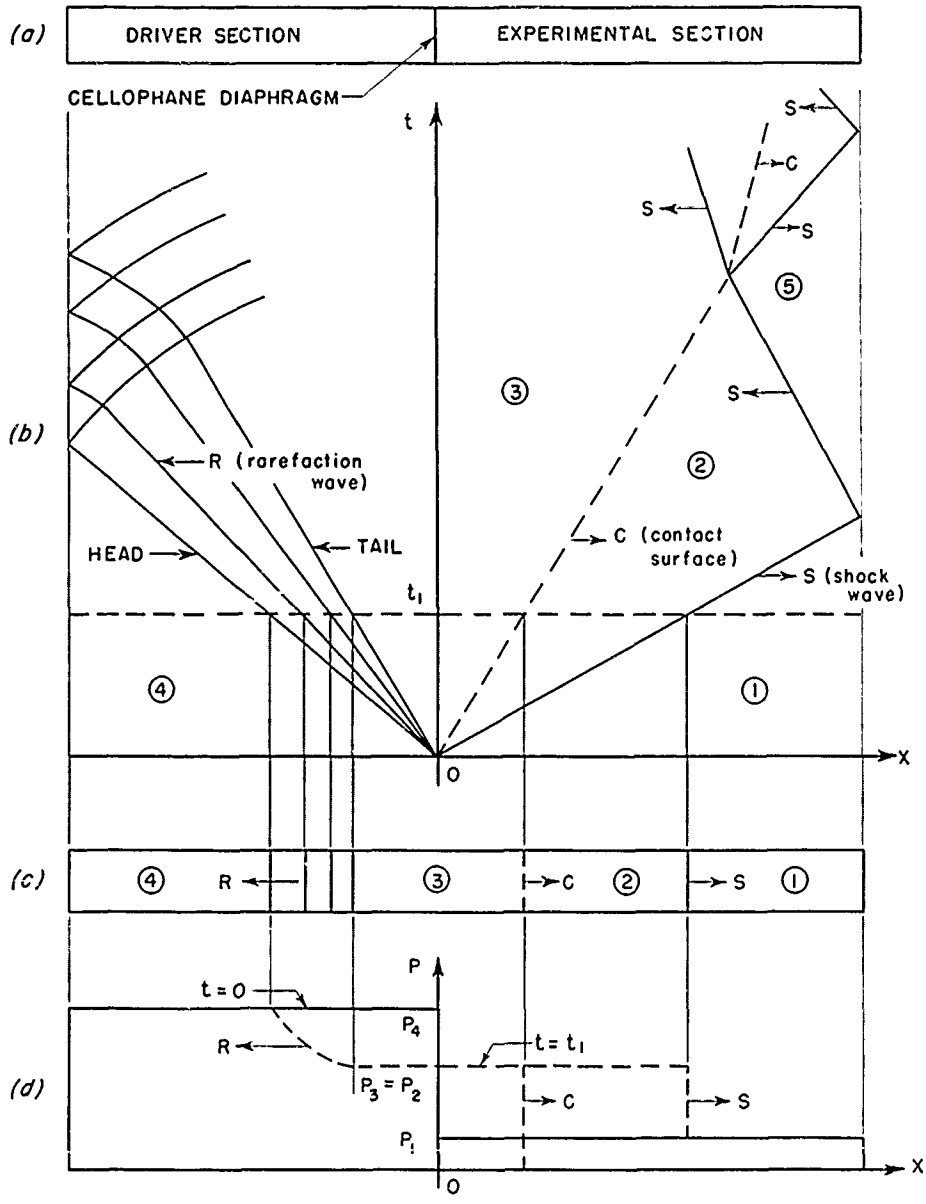

(a) Shock Tube Before Diaphragm is Broken
(b) Wave Diagram in t - x Plane
(c) Waves in Shock Tube at $t = t_1$
(d) Pressure Distribution at $t = t_1$

WAVE SYSTEM IN SHOCK TUBE

Figure 13.

accelerates the expanded gas in a direction opposite to the motion of R. The movement of these waves is represented in Figure 13b, in which the horizontal axis corresponds to position along the shock tube and the vertical axis represents time. On such a graph the motion of a wave can be followed in time along lines whose slopes correspond to the wave speeds. The centered rarefaction wave is represented by a pencil of characteristic lines radiating from the origin. Both the shock and rarefaction waves undergo normal reflection at the ends of the tube. The reflected shock wave reacts with the contact surface, producing a transmitted shock wave and either a reflected shock wave or a reflected rarefaction wave depending on the acoustic impedance in the gas regions involved. As time goes on the various waves continue to interact with each other and to be reflected from the ends of the shock tube. In an actual shock tube this activity quickly subsides because of viscous effects, heat loss at the walls, and other dissipative effects.

In (b) and (c) of Figure 13 several regions of uniform flow are labelled with circled numbers. Regions 1 and 4 refer to the initial state of the experimental and driver gases, respectively. In region 2 we have experimental gas which has been compressed and heated by the shock wave. The driver gas which has been expanded and cooled by the rarefaction wave is in region 3. It is evident that if $T_1 = T_4$, then $T_3 < T_2$. This means that the contact surface is a temperature discontinuity in addition to being a boundary between gases of different origin. The particle speed and pressure, however, are the same on both sides of the contact surface. This "surface" generally broadens into a region in which the gases are mixed by turbulence generated by the diaphragm burst. Between regions 3 and 4 there is a transition zone which spreads with time. The head and tail of this zone advance at sonic speeds (relative to the gas) appropriate to regions 4 and 3, respectively. In region 5 we have gas which has been brought to rest by the reflected shock

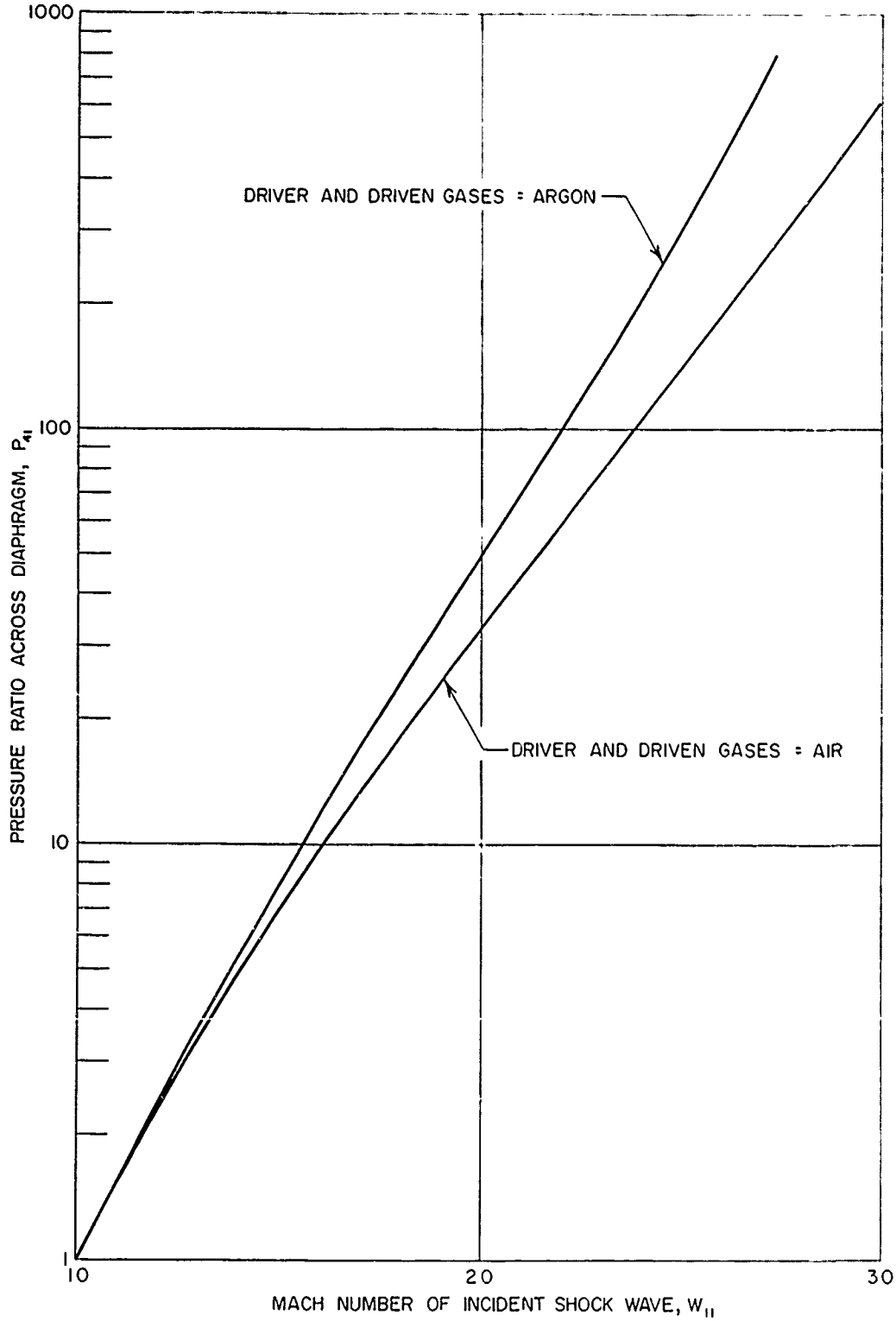

Figure 14. Relation of Incident Shock Wave Mach Number to Pressure Ratio Across Diaphragm.

wave and which has been further compressed and heated by it. Figure 13c and 13d illustrate the situation at an arbitrary time $t = t_1$ before the shock wave is reflected.

Figure 14 shows the relation between the Mach number of the incident shock wave and the pressure ratio across the diaphragm for the cases in which both driver and driven sections of the shock tube were filled with air and with argon. These curves were used to select the shock tube pressures to yield the desired shock wave strength.

APPENDIX B. STATISTICAL ANALYSIS OF EXPERIMENTAL DATA

The mean value, variance, and standard deviation for each group of experiments were calculated according to standard procedures:

The mean value is

$$\bar{x}_i = \frac{\sum_j x_{ij}}{n_i}$$

where i = index of experimental group

j = index for individual readings within a group

n_i = number of readings in Group i

The estimated variance is

$$V_i = s_i^2 = \frac{\sum_j \left(\bar{x}_i - x_{ij}\right)^2}{\varphi_i}$$

where $\varphi_i = n_i - 1$ represents the number of degrees of freedom in Group i.

The estimate of the standard deviation is s_i, or simply the square root of the variance estimate.

Analysis of Data in Table 1.

In the above calculations, no account is taken of the inter-relation of experiments among various groups. When the data consists of several groups of relatively few experiments it is useful to check whether one is justified in using all the data to obtain a better estimate of error than is possible from individual groups. In Table 1, the hypothesis that the mean squares, V_i, are estimates of the same variance and may therefore be used as an estimate of error was tested by Bartlett's criterion. (See pages 286-289 of Reference 12).

This test requires the calculation of the following five quantities, (i) to (v):

(i) $A = \frac{1}{3(k-1)}\left(\sum_i \frac{1}{\varphi_i} - \frac{1}{\varphi} \right)$ where k is the number of mean squares, i.e. the number of groups in Table 1, and φ is the total number of degrees of freedom, $\sum_i \varphi_i$.

(ii) $f_1 = k - 1$

(iii) $f_2 = (k + 1)/A^2$

(iv) $b = f_2/(1 - A + 2/f_2)$

(v) $M = \varphi \ln V - \sum_i \varphi_i \ln V_i$, where $V = \sum_i V_i$.

One then applies the F-test (see p. 29 of Reference 12.) with f_1 and f_2 degrees of freedom to the ratio $r = f_2 M/[f_1(b - M)]$. Note that f_1 corresponds to the number of degrees of freedom of the greater variance.

The F-test is a method for comparing two sample variances. If s_1^2 and s_2^2 based on φ_1 and φ_2 degrees of freedom respectively are independent estimates of the variance, σ^2, of a normally distributed universe, then the ratio σ_1^2/σ_2^2 is distributed as F with φ_1 and φ_2 degrees of freedom. As indicated above, the Bartlett criterion applies the F-test to the ratio r, with f_1 and f_2 degrees of freedom. The data of Table 1 yield

$r = 2.06$

$f_1 = 4$

$f_2 = 175.8$

From tables of the F distribution it was found that values of r equal to, or higher than, the above value could occur by chance 5 to 10 times out of 100 if the variabilities of each group were truly alike. It was concluded, therefore, that the variability was the same for all data in Table 1.

An analysis of variance was carried out next, to determine whether there is any significant difference among the means of the various intermediate groups. The method followed is that given in Section 7.24, page 327 of Reference 13. The model on which this analysis is based assumes that the average value for a particular group is the combination of an overall mean plus a variation from this overall mean, the variation being an effect due to the characteristic associated with that group.

$$\bar{x}_i = \mu + \xi_i$$

Two estimates of variance are made: (1) The "within groups" estimate yields an estimate of the basic variance σ^2; and (2) the "between groups" estimate includes an additional contribution due to σ_ξ^2, the variance of the population of effects from which the ξ_i were drawn. Application of the F-test to the ratio of the two estimates of variance checks the hypothesis $\sigma_\xi^2 = 0$ and enables us to determine whether the various ξ_i are significantly different.

The details of the calculations are illustrated in the following "Analysis of Variance" table:

Source of Estimate	Corrected Sum of Squares	Degrees of Freedom	Mean Square	Average Mean Square
Between groups	$S_i = \sum_i n_i(\bar{x}_i - \bar{x})^2 = 2370.9895$	$k - 1 = 4$	$\frac{S_i}{k-1} = 592.75$	$\sigma^2 + \frac{(N^2 - \sum_i n_i^2)}{(k-1)N}\sigma_\xi^2$
Within groups	$S_{ij} = \sum_{ij}(x_{ij} - \bar{x}_i)^2 = 537.148$	$\sum_i n_i - k = 15$	$\frac{S_{ij}}{N-k} = 35.81$	σ^2
Total	$S = \sum_{ij}(x_{ij} - \bar{x})^2 = 2908.1375$	$N - 1 = 19$	—	—

The variables not previously used are defined as follows:

k = number of groups

n_i = number of observations in group i

$\bar{x} = \frac{\sum_{ij} \bar{x}_{ij}}{N}$ = overall average

$N = \sum_{i=1}^{n} n_i$

S, S_i, S_{ij} = corrected sums of squares, as defined in the second column of the above table.

To test the hypothesis that there is no appreciable variation between the average values of the different groups we form the variance ratio

$$\frac{592.75}{35.81} = 16.6$$

At the 0.5% level, for 4 and 15 degrees of freedom, F has the value 5.80. As this is exceeded by 16.6 the conclusion is that our variance ratio can occur by chance, if there is no difference between groups, in less than 1/2% of the cases. Hence, we can assume that there are significant differences among the groups.

To establish which groups were significantly different a "gap and straggler" procedure modeled after Reference 14 was employed. The groups were ordered according to the means and the calculations indicated in the following table were carried out.

Group	a	b	c	d	e
$\bar{x}_i$	-0.48	4.82	20.0	22.5	26.75
Δ		5.3	15.18	2.5	4.25
φ		9	7	3	4
σ_Δ^2		3.9789	5.1157	11.9367	8.9525
σ_Δ		1.99	2.26	3.45	2.99
"t"		2.66	6.72	0.72	1.42
P		~ 2.5%	< 1/2%	> 50%	10% to 25%

Δ is the difference between successive means.

φ is the sum of the degrees of freedom in each pair of groups examined.

σ_Δ^2 is obtained by dividing φ into the best estimate of the overall variance σ^2, which we found above to have the value 35.81

$$t = \frac{\Delta}{\sigma_\Delta}$$

P is the probability that t would by chance have the value calculated, under the hypothesis that the corresponding pairs of successive means are not significantly different. P can be found from a t-distribution table, such as Table III, p 696, of Reference 13.

The conclusions to be drawn are that the mean of Group b significantly exceeds the mean of Group a; Group c is significantly greater than Group b; Groups c and d are not significantly different; Group e can be said to exceed Group d with only a low level of confidence.

Finally, we can show how the 95% confidence limits for the means were calculated. An improved estimate of the variance of each group was obtained as follows:

$$\sigma_{\bar{x}_i}^2 = \frac{35.81}{n_i}$$

where 35.81 is the best estimate of the overall variance and n_i is the number of observations in Group i. At the 5% level, with 15 degrees of freedom, t lies within the limits ± 2.13. The 95% confidence limits are given, therefore, by

$$\bar{x}_i \pm 2.13\ \sigma_{\bar{x}_i}$$

The true mean is expected to lie within these limits with a confidence of 95%. (See Reference 12, page 21.)

Analysis of Data in Table 2

The seven groups of experiments in Table 2 were analyzed for equal variability by Bartlett's criterion as in the analysis of data in Table 1. We obtained

$$f_1 = 6$$

$$f_2 = 461.78$$

$$r = 2.48$$

The F-distribution tables show that this value of r will occur by chance, if the variabilities are truly alike, only 1 to 5 times out of a 100. Hence, it is not likely that this value of r is a chance result, and we must conclude that the various groups in Table 2 do not have equal variability.

The analysis of variance to determine whether there is any significant difference among the means of the various groups proceeded along the same lines followed in the analysis for Table 1, except that the individual observations in Table 2 were weighted in proportion to the reciprocal of their variance. This was done according to Reference 13, Section 6.27, page 243.

The weighted, corrected sum of squares within each group (WCSS) was calculated according to the formula:

$$\text{WCSS} = w_i \sum_j x_{ij}^2 - \frac{w_i \left(\sum_j x_{ij}\right)^2}{n_i}$$

where $w_i = \frac{1}{s_i^2}$,

and the other quantities are as previously defined.

The total corrected sum of squares was obtained from the formula:

$$\text{Total CSS} = \sum_i w_i \sum_j x_{ij}^2 - \frac{\left(\sum_i w_i \sum_j x_{ij}\right)^2}{\sum_i n_i w_i}$$

The "Analysis of Variance" table takes the form:

Source of Estimate	Corrected Weighted Sum of Squares	Degrees of Freedom	Mean Square
Total	907.899	28	--
Within	27.933	22	1.2697
Between	879.966	6	146.66

The only difference between this table and the corresponding table given above occurs in the second column, where the corrected sums of squares have been replaced by "weighted" corrected sums. The corrected sums of squares between is obtained as the difference between the total and within values.

The ratio of the mean square between to the mean square within is 146.66/1.2697 = 115. The F-test shows that it is extremely unlikely that this ratio would be obtained by chance if there were no significant difference among the means of the various groups. Hence, we conclude that significant differences do exist.

The groups were ordered according to mean value and analyzed for significant differences among successive pairs of groups using the same procedure as was applied to the data of Table 1, except that it was necessary to consider individual variabilities instead of an overall value. The quantity σ_{Δ}^2 for two successive groups, i and i + 1, was calculated as follows:

$$\sigma^2_{\Delta_{i,i+1}} = \frac{s_i^2}{n_i} + \frac{s_{i+1}^2}{n_{i+1}}$$

Among successive pairs, only Groups k and l turned out to be significantly different. Although, it is likely that significant differences exist among non-successive pairs of experimental groups, the data did not seem to justify more elaborate analysis to establish the differences statistically.

The 95% confidence limits were also calculated by the same procedure applied to the data of Table 1, except that individual variances, instead of an overall variance, were considered. The only change appeared in calculating the quantity $\sigma^2_{\bar{x}_i}$, which was defined as:

$$\sigma^2_{\bar{x}_i} = \frac{s_i^2}{n_i}$$

Analysis of Data in Table 3

This analysis was carried out according to the method of multiple regression, Reference 13, Section 6.3, page 245. Each observation of α was assumed to be from a normal distribution with mean

$$y = a + bM + cC + d(MC)$$

and variance σ^2. The quantities M, C, and MC are variables which refer respectively to the magnetic field, short circuiting of the collecting plates, and the combination of magnetic field and short circuiting. The coefficients b, c, d which measure the influence of the corresponding variables on the observed value of the dependent variable are determined by the method of least squares.

The coefficients and the 95% confidence limits were found to have the following values:

$$a = 8.82 \pm 2.96$$
$$b = 3.60 \pm 3.42$$
$$c = -0.20 \pm 4.20$$
$$d = 0.15 \pm 6.38$$

We see that b is clearly different from zero, and we conclude that the magnetic field definitely influences the value of α. However, the coefficients c and d are not clearly defined, and we cannot on the basis of this analysis conclude that the corresponding variables have a significant effect on the value of α.

The best unbiased estimate of the variance σ^2 was given by

$$s^2 = \frac{\sum_{ij}\left(y_{ij}-\bar{y}_i\right)^2}{N-3} = 8.78$$

where N = 27 is the total number of observations in Table 3 and the summation is carried out over all observations. At the 5% level and with 23 degrees of freedom the "t" value is 2.069. Using this value of t the 95% confidence limits for the mean of each of the four groups of experiments in Table 3 were calculated with the formula:

$$\text{Confidence Limits} = \pm t\sqrt{\frac{s^2}{n_i}}$$

where n_i is the number of observations in Group i.

Analysis of Data in Table 5

In Table 5 we were interested in seeing whether there is any significant difference between $(V_{12}-V_{23}) = X$, and $(V_{23}-V_{34}) = Y$. The following procedure was applied to the group of experiments in which the collecting plates were open circuited.

The differences $\Delta_i = Y_i - X_i$ were calculated, and their mean value was found to be $\bar{\Delta} = 0.325$. The estimated variance of the mean difference is

$$S^2_{\bar{\Delta}} = \frac{\sum_i\left(\Delta_i-\bar{\Delta}\right)^2}{n_i(n_i-1)} = 0.1528$$

where $n_i = 8$, is the total number of experiments in the group. The ratio of the mean, $\bar{\Delta} = 0.325$, to its standard deviation, $\sqrt{S^2_{\bar{\Delta}}} = 0.1528$, was found to be 0.83. To check the null hypothesis, that $\bar{\Delta}$ is zero, or that there is no difference between X and Y, we used the Student "t" tables for 8 degrees of freedom. The table showed that the ratio with a value of 0.83, or higher, could occur by chance with a probability considerably exceeding 25% if the null hypothesis

were true. Hence we concluded that there is no significant difference between $(V_{12} - V_{23})$ and $(V_{23} - V_{34})$.

It appeared quite clear, even omitting the calculations, that the same conclusion is applicable to the second group of experiments in Table 5, the group in which the collecting plates were short circuited.